Life-cycle-related gene expression patterns in the brown algae

Pélagie Ratchinski[1], Olivier Godfroy[2], Benjamin Noel[3], Jean-Marc Aury[3], J. Mark Cock[1,*]

[1]Sorbonne Université, CNRS, Algal Genetics Group, Integrative Biology of Marine Models Laboratory, Station Biologique de Roscoff, Roscoff, France
[2]Sorbonne Université, CNRS, CMAR, Integrative Biology of Marine Models Laboratory, Station Biologique de Roscoff, Roscoff, France
[3]Génomique Métabolique, Genoscope, Institut François Jacob, CEA, CNRS, Université Evry, Université Paris-Saclay, Evry 91057, France
*Corresponding author. E-mail address: cock@sb-roscoff.fr (J.M. Cock)

Keywords: brown algae, early development, *Dictyota dichotoma, Ectocarpus* species 7, gene clustering, life cycle, seaweed, transcriptomics

Abstract

Brown algae are important primary constituents of marine coastal ecosystems, characterised by complex life cycles and various levels of complex multicellular development. However, the molecular processes that underlie development and life cycle progression in the brown algae remain poorly understood. In this study, pairwise comparisons of gametophyte and sporophyte transcriptomes across ten diverse brown algal species showed that the total number of genes exhibiting generation-biased or generation-specific expression in each species was correlated with the degree of dimorphism between life cycle generations. However, analysis of gene ontology terms assigned to the generation-biased/generation-specific genes indicated that each generation (i.e. the sporophyte and the gametophyte) also has characteristic broad life-cycle-related features that have been conserved during evolution. A more detailed analysis of *Ectocarpus* species 7, identified progressive transcriptome changes over its entire life cycle with a particularly marked change in transcriptome composition during the first day of sporophyte development, characterised by downregulation of flagellar and transcription factor genes and upregulation of a subset of translation genes. Comparison with a similar transcriptomic time series for the evolutionarily-distant (about 250 My) brown alga *Dictyota dichotoma* indicated considerable conservation of co-expressed gene modules between the two species, particularly for modules that were enriched in genes assigned to evolutionarily-conserved functional categories. This study therefore identified broad life-cycle- and development-related patterns of gene expression that are conserved across the brown algae.

Introduction

Brown algae are major primary components of diverse and widespread coastal ecosystems, often forming extensive underwater forests (Bringloe *et al.*, 2020; Eger *et al.*, 2023). The group includes large (up to 50 metres) multicellular organisms that rival many land plant species in complexity. From a developmental point of view, brown algae are particularly interesting because they evolved complex multicellularity independently of land plants and animals (Cock *et al.*, 2010). Taxonomically, these seaweeds are grouped into the class Phaeophyceae, which is a major taxon within the stramenopiles, and therefore very distant, phylogenetically, from the Archaeplastida and the Opisthokonta lineages that gave rise to land plants and animals, respectively. Consequently, brown algae represent interesting alternative systems to investigate the evolution and molecular bases of developmental processes.

Most brown algae have haploid-diploid life cycles involving an alternation between two independent multicellular generations, the sporophyte and the gametophyte (Cock *et al.*, 2014). These seaweeds are therefore capable of deploying two different multicellular developmental programs, each at the

appropriate stage of their complex life cycles. The relative sizes of the two life cycle generations varies considerably across brown algae, with either the sporophyte or the gametophyte being the largest generation (dimorphism) or the two generations having very similar sizes and morphologies (isomorphy). Transitions between life cycles with different degrees of dimorphism have occurred frequently during the evolution of the brown algae (Cock *et al.*, 2014). Variations on this central sexual life cycle have been observed in culture for several species and these variations can provide insights into the mechanisms that control life cycle progression. For example, if gametes of the filamentous brown alga *Ectocarpus* fail to fuse with a gamete of the opposite sex to form a zygote, they are often capable of germinating parthenogenetically to produce a haploid partheno-sporophyte that is morphologically and functionally indistinguishable from a diploid sporophyte (Müller, 1967). The existence of these haploid sporophytes indicates that life cycle generation identity is not determined by ploidy in this species and is therefore presumably under genetic control.

The occurrence of two multicellular generations during the life cycles of most brown algae allows genetic screens to be carried out for mutations that cause switching between the development programs of the two generations, i.e. mutations that lead to deployment of the incorrect program at a specific point in the life cycle (Coelho and Cock, 2020). Using this approach, two three-amino-acid-loop-extension (TALE) homeodomain transcription factor (HD TF) genes, *OUROBOROS (ORO)* or *SAMSARA (SAM)*, have been show to be necessary for deployment of the sporophyte generation developmental program in *Ectocarpus* (Coelho *et al.*, 2011; Arun *et al.*, 2019). Mutations in either of these genes suppresses the ability of the alga to produce a functional sporophyte, leading to deployment of the gametophyte program at life cycle stages where a sporophyte should normally be produced. In addition, *Ectocarpus* sporophytes have been shown to produce a diffusible factor that can induce sporophyte development in gametophyte initial cells (Arun *et al.*, 2013; Yao *et al.*, 2021). The diffusible factor does not induce life cycle generation switching in *oro* or *sam* mutant gametophyte initial cells, indicating that it acts upstream of ORO and SAM (Arun *et al.*, 2013, 2019).

The genetic pathways that underlie the deployment of the sporophyte and gametophyte developmental programs in brown algae are still poorly understood. Mutations in a small number of genes have been shown to lead to developmental defects in *Ectocarpus* (Macaisne *et al.*, 2017; Godfroy *et al.*, 2017, 2023) but a mutation in the *IMMEDIATE UPRIGHT* gene is the only lesion that specifically affects the development of one of the two generations (Peters *et al.*, 2008). Transcriptomics has been used to identify genes that are differentially expressed between the two generations in *Ectocarpus* (Arun *et al.*, 2019; Lipinska *et al.*, 2019; Bourdareau *et al.*, 2021). These transcriptomic analyses focused on comparisons of adult sporophyte and gametophyte thalli and have allowed the identification of several hundred genes that are differentially expressed between these two stages of development. However, the analyses were not designed to detect genes that are important during early development and do not provide any information about the kinetics of gene expression over development. In recent years, several detailed studies have generated gene expression data for multiple developmental stages or organs for several different brown algal species (Pearson *et al.*, 2019; Shao *et al.*, 2019; Shan *et al.*, 2020; Zhang *et al.*, 2021; Graf *et al.*, 2022; Liang *et al.*, 2023; Uji *et al.*, 2024), including a transcriptomic analyses of early stages of *Dictyota dichotoma* sporophyte development (Bogaert *et al.*, 2017). This latter study detected changes in the transcriptome less than one hour after fertilisation, providing evidence for *de novo* transcription in the zygote, and identified a set of genes with diverse functions that were differentially regulated during early sporophyte development.

In the current study, transcriptomic data, recently generated by the Phaeoexplorer project (Denoeud *et al.*, 2024), was used to analyse differential gene expression between the adult sporophyte and gametophyte generations of a broad range of brown algae. The proportion of genes that showed generation-biased or generation-specific expression across these two stages was correlated with the

level of dimorphism between the two generations indicating that the differentially expressed genes are primarily linked to morphological differentiation. However, analysis of gene ontology terms also identified underlying, life-cycle-related characteristics that have been conserved during evolution, with general classes of gene function being conserved across sporophytes of the ten species, and different general classes of gene function being conserved across the gametophytes. In addition, analysis of transcriptomic data corresponding to multiple stages of the *Ectocarpus* life cycle, generated by combining published RNA sequencing (RNA-seq) data with newly-generated timepoints, identified co-expression modules containing genes with specific expression patterns during life cycle progression. This analysis identified several modules that exhibited marked expression pattern changes during early sporophyte evolution, providing insights into key genetic events during this period. Comparison with a set of gene co-expression modules generated for *D. dichotoma* identified conserved features shared by these two distantly related brown algal species.

Results

Across the brown algal lineage, the proportion of generation-biased genes is correlated with the degree of life cycle dimorphism

RNA-seq data for the adult sporophyte and gametophyte generations of ten different brown algal species (Figure 1A, Table S1) were analysed to obtain a broad overview of generation-biased gene expression across the brown algae. The species analysed had markedly different haploid-diploid life cycles, ranging from sporophyte dominance, through sporophyte-gametophyte isomorphy to gametophyte dominance (Figure S1). As previously observed in a smaller-scale analysis that looked at four different brown algal species (Lipinska *et al.*, 2019), the proportion of generation-biased/generation-specific genes (see Materials and Methods for definitions of generation-biased and generation-specific genes) identified in each species was positively correlated with the degree of intergenerational dimorphism (Figure 1B, Table S2). Surprisingly, however, species with strongly dimorphic life cycles had greater numbers of both sporophyte- and gametophyte-biased/specific genes, indicating either that gene downregulation plays an important role in the establishment of dimorphic generations or that there is also cryptic complexification of the more morphologically simple generation.

We also noted that, depending on the species, only between 10% and 24% (Table S2) of genes were expressed during one generation but not the other (defined for this analysis as mean TPM 1 for one generation but mean TPM <1 in the other generation), indicating that most genes are expressed during both generations of the life cycle. There is therefore considerable scope for many genes to have functions during both generations of the life cycle. In terms of selection, this observation indicates that most genes are potentially directly exposed to purifying selection during the haploid phase (where there is no effect of masking by a second allele of each locus) and few genes are expressed solely in a diploid context where masking would be most effective.

The sporophyte and gametophyte generations express characteristic general functional categories of genes

To evaluate the degree of conservation of generation-biased/specific gene sets across the ten brown algal species an orthogroup analysis was carried out (Table S3) using Orthofinder (Emms and Kelly, 2019). Pairwise comparisons of generation-biased/specific genes that had orthologues in all ten species indicated that the sets of generation-biased/specific genes were poorly conserved across species, even for closely-related species such as the two *Saccharina* spp. (Figure 1C). None of the orthogroups exhibited conserved generation bias across all the ten species. The lack of conservation of generation-biased/specific gene sets across species is in line with observations made in the earlier study that compared four brown algal species (Lipinska *et al.*, 2019). However, despite the poor

conservation of generation-biased/specific expression at the individual gene level, analysis of enriched gene ontology terms across the entire generation-biased/specific gene sets from the ten studied brown algae identified distinct sets of enriched terms for both the sporophyte-biased/specific and the gametophyte-biased/specific genes (Figure 2) and the general classes of enriched gene ontology term were conserved for each individual generation across the ten species. For example, the sporophyte-biased/specific gene sets tended to be enriched in genes with predicted functions related to membrane transport and metabolism whereas the gametophyte-biased/specific gene sets tended to be enriched in genes with predicted functions related to flagella biosynthesis and function, protein biosynthesis and DNA-related functions (Figure 2). These analyses identified an underlying similarity between sporophyte generations across species and between gametophyte generations across species, and indicated that these generation-characteristic patterns of gene expression are present even in species where the two generations are isomorphic or nearly isomorphic.

Changes in gene expression patterns over the course of the *Ectocarpus* species 7 life cycle reflect the cyclic transitions between life cycle stages

The above analyses specifically provided information about gene regulation patterns underlying morphological and functional differences between the adult stages of the two generations. To obtain a broader view of gene expression during the life cycle, RNA-seq samples corresponding to multiple stages of the *Ectocarpus* species 7 life cycle were analysed: replicate samples corresponding to two very early stages (24 h and 48 h after gamete release; Figure S2) of sporophyte development were generated and combined with publicly-available samples corresponding to eight other stages of the life cycle (Table S1).

In a Principal Component Analysis (PCA) the dispersion of the samples corresponding to these ten life cycle stages mirrored the cyclic organisation of the alga life cycle (Figure 3A). Together, the two main axes explained 57% of the observed variability, with adult stages grouping together at one end of the first axis and early stages localised at the other end. The second axis approximately separated the sporophyte and gametophyte phases of the life cycle. The PCA pattern indicated gradual changes in transcriptome content between each stage of the life cycle, so that successive stages possessed overlapping but different transcriptomes.

The first day of sporophyte development corresponds to a major shift in the pattern of gene expression

The PCA also indicated marked differences between the gamete stage and all the other stages of the life cycle (Figure 3A). To further investigate this observation, the Trendy R package (Bacher *et al.*, 2018) was used to calculate the fit of segmented regression models to individual gene expression patterns in order to identify individual genes that best matched the overall pattern of regression breakpoints. When this approach was applied to the sporophyte developmental series, a good regression fit ($R^2 > 0.5$) could be calculated for 5,196 genes and 32% of these genes exhibited a change in expression (i.e. a regression breakpoint) during the transition from the gamete stage to the sporophyte initial cell (24 h) stage (Figure 3B), indicating that this transition involves a major shift in the pattern of gene expression.

To complement the above analysis, DESeq2 (Love *et al.*, 2014) was used to identify genes that were differentially expressed between the free-swimming gamete and the sporophyte initial cell stage. This analysis detected 10,955 differentially expressed genes, corresponding to 4,372 and 6,583 significantly up- and down-regulated genes, respectively. These differentially expressed genes represent 58% of the total number of genes in the *Ectocarpus* species 7 genome (Figure 3C). For comparison, when adult sporophytes and gametophytes stage were compared (Figure 1B), 3,726

upregulated and 2,577 downregulated genes (35% of the total number of genes overall) were detected. The DESeq2 analysis therefore supported the conclusion that a marked change in gene expression pattern occurred between the free-swimming gamete stage and the sporophyte initial cell stage.

Interestingly, in the comparison between gametes and the sporophyte initial cell, the mean fold change in transcript abundance for downregulated genes at the transition between free-swimming gamete and initial cell was significantly higher than the mean fold change for genes that were upregulated at this transition (Wilcoxon rank sum test *p*-values < 2.10^{-16}; Figure 3D). This observation suggested narrower expression ranges for the downregulated genes and this hypothesis was supported by a comparison of tau values (a measure of breadth of expression) for the downregulated and upregulated genes, which showed that the downregulated genes had significantly higher tau values (Wilcoxon rank sum test *p*-values < 2.10^{-16}; Figure S3). A comparison across the ten life cycle stages also showed that 61% of the genes downregulated at the gamete to initial cell transition were most strongly expressed at the gamete stage (data in Tables S4, S5).

Analysis of gene co-expression modules indicated coordinated regulation of genes associated with several cellular processes

To further analyse gene expression patterns over the life cycle, a weighted correlation network analysis (WGCNA) approach (Langfelder and Horvath, 2008) was used to group genes according to their patterns of expression across the ten life cycle stages. Using a cut-off of normalised counts ⍰45 (DESeq2 analysis), 16,077 of the 18,370 *Ectocarpus* species 7 genes were classed as being significantly expressed at at least one stage of the life cycle. Of these genes, 14,277 could be assigned to one of 23 gene expression modules, which varied in size from 42 to 2,414 genes (Figures S4, 4, Table S6). The modules were given arbitrary colour names (Figure 4F). The 24th "grey" module groups the 1,800 genes that were not assigned to a co-expression module (Figure 4F, Table S6).

The 23 gene co-expression modules were analysed for enriched gene ontology (GO) terms (Figures 5 and S5). For 11 of the 23 gene co-expression modules, the set of enriched GO terms were sufficiently related to allow a general biological function to be manually assigned to the module (Figure 4A). These modules indicated that at least a proportion of the genes involved in several cellular processes (photosynthesis, DNA modification, flagella biosynthesis/function, transcription and translation) are co-ordinately regulated during the life cycle.

The PCA and differential expression analyses described above provided evidence for a large-scale modification of the transcriptome during the transition between the gamete and sporophyte initial cell stage. As expected, changes in expression level at this transition strongly influenced the grouping of genes into expression modules (Figure 4F) and several modules were enriched in genes that had been identified as differentially expressed at this first transition (Figure 4C). The following two sections will focus on these modules to further characterise this important early developmental transition.

Sporophyte down-regulated gene modules highlighted DNA- and flagella-related functions in gametes

Seven modules were significantly enriched in genes that were downregulated during the transition from gametes to the sporophyte initial cell (Figure 4C, Table S6). For three of these modules, “pink”, “salmon” and “turquoise”, the genes were also upregulated during the gametophyte stages (Figure 4D). The “pink” module was enriched in gene ontology terms related to nucleosome assembly (Figure S5) and the “salmon” module, which contained a large number of monoexonic genes, was enriched in genes predicted to have DNA-related functions (enriched gene ontology terms included “DNA

integration", "DNA recombination", "DNA repair", "DNA helicase" and "telomere maintenance"; Figure S5). The "turquoise" module, which had an expression profile very similar to that of the "salmon" module (Figure 4D), was enriched in genes with predicted functions related to the flagella (enriched gene ontology terms included "dynein complex", "cilium", "BBSome", "microtubule-based movement", "axonemal dynein complex assembly", "cilium movement" and "microtubule motor activity"), and therefore presumably important for gamete motility (Figure S5). The upregulation of "turquoise" module genes in gametophytes is probably explained by the production of flagellated gametes in the gametangia of fertile thalli although it is not clear why the genes were also expressed a quite a high level in pre-fertile, adult gametophytes. It is possible that transcripts already accumulate at this stage to prepare for the production of large numbers of gametes at fertility or that some of these genes are also involved in other cellular functions, for example related to the cytoskeleton.

Cell-wall biosynthesis functions were not significantly enriched in the "turquoise", "salmon" and "pink" modules but these modules contained the majority of annotated genes from two families of carbohydrate-active enzymes (CAZymes), the GT23 family (four genes in the "turquoise" and two genes in the "salmon" module out of ten genes in total) and the PL41 family (nine genes in the "turquoise" module, five genes in the "salmon" module and three genes in the "pink" module out of 22 expressed, annotated PL41 genes; Figure S6). The GT23 family is predicted to encode fucosyltransferases, which would transfer fucosyl groups onto chitin oligosaccharides or glycoproteins, and the PL41 family contains mannose-specific alginate lyases (Inoue and Ojima, 2019; Mazéas *et al.*, 2024). While the role of GT23 enzymes in gametes is unclear, it is possible that the polysaccharide depolymerisation action of PL41 lyases may facilitate gamete release from plurilocular sporangia in a manner analogous to the actions of pectate lyases and rhamnogalacturonan lyases during fruit ripening in land plants (Méndez-Yañez *et al.*, 2020; Uluisik and Seymour, 2020; Al-Hinai *et al.*, 2024).

The remaining four modules that were significantly enriched in genes downregulated during the transition from the gamete to the early sporophyte ("blue", "green", "red" and "grey60") did not exhibit gene upregulation during the gametophyte generation (Figure 4C, D, Table S6). No significant GO term enrichment was detected for the "blue" and "green" modules. The "red" and "grey60" modules were enriched in transcription factors and related GO terms such as "DNA-binding domain" (Figure S5). To investigate this point further a recently established dataset of 325 transcription-associated proteins (TAPs) for *Ectocarpus* species 7 (Denoeud *et al.*, 2024) was enriched with the 90 Esv-1-7 domain proteins (Macaisne *et al.*, 2017) from this species (Table S5, Figure S7), as the latter have been hypothesised to function as zinc finger transcription factors (Macaisne *et al.*, 2017), and the expression of these genes analysed in gametes. Transcripts of approximately a third of the genes (147) in this transcription-associated dataset were more abundant in gametes than at the sporophyte initial cell stage (24 h) but the proportion was similar to the proportion for all the genes in the genome indicating that there was not an overall enrichment of the gamete transcriptome in transcription-associated genes.

Taken together, analysis of the seven modules highlighted the importance of DNA-related functions, including nucleosome assembly and transcription, and flagella-related functions in gametes.

Subsets of translation-related genes are upregulated in the sporophyte initial cell but the gamete already expresses some translation-related and photosynthesis genes

Nine modules were significantly enriched in genes upregulated during the transition between gametes and the sporophyte initial cell (Figure 4C, Table S6). Most of the nine modules could not be clearly associated with a general cellular process but three ("cyan", "magenta" and "greenyellow") were enriched in functions related to translation (Figures 4A, 5). These three modules exhibited very

similar expression profiles (Figure 5A) but were enriched in different classes of translation-related gene (Figure 5B-E). The "greenyellow" module contained the RNA polymerase I gene which synthesises rRNA and was enriched in GO terms related to "nucleolus", "small-subunit processome", "ribosome large subunit assembly", "ribosome biogenesis" and "rRNA processing". This module was therefore essentially related to the biosynthesis of the ribonucleic component of the ribosome (Figure 5D). The "cyan" and "magenta" modules were enriched in GO terms such as "tRNA aminoacylation for protein translation", "tRNA processing", "translation initiation" (Figure 5E). These two clusters included 25 of the 49 aminoacyl-tRNA-transferases annotated in the *Ectocarpus* species 7 genome, and also included a number of genes related to transcription initiation (Figure 5C). Notably, the "cyan" module included nine eIF3-subunit-encoding genes out of a total of 15 annotated genes in the genome (Figure 5C). Interestingly, the "cyan" and "greenyellow" modules were enriched (p <0.05 clusterProfiler) in genes with a mitochondrial targeting sequence (Figure 4B), whereas the "magenta" module was enriched (p<0.05 clusterProfiler) in genes that encode proteins targeted to the plastid. The plastid-targeted proteins had predicted functions other than photosynthesis (e.g. translation and transport).

The "cyan", "greenyellow", and "magenta" modules clustered together based on their average expression profiles (Figure 4F), suggesting that the three groups of translation-related functions share some level of co-expression. Taken together, the gene content of these three clusters suggest that there is a marked increase in translation in the initial cell compared to the gamete, both in the cytosolic and the organellar compartments. Importantly, however, not all translation-related genes exhibited marked upregulation during the transition from the gamete to the initial cell stage. For example, the transcripts of the many ribosomal-protein-encoding genes that were grouped in the "purple" module were already present in gametes at relatively high levels (Figures 5B, S8). The ribosomal protein genes are an interesting case because, whilst the majority of these genes were assigned to the "purple" module, corresponding essentially to constitutive expression, a minority of the members of this broad family exhibited more complex expression patterns and were assigned to other modules (Figures 5B, S8). In general, this latter minority of genes tend to encode proteins that are located in close vicinity in the P-stalk within the ribosome (Figure S9). The functional significance of this clustering is unclear but it has been proposed that the P-stalk influences translation fidelity and the pool of mRNAs associated with the ribosome (Wawiórka *et al.*, 2017; Dopler *et al.*, 2024). We also noted that ribosomal protein genes with non-constitutive expression patterns tended to have paralogues that were constitutively expressed (Figure S8). Interestingly, cytosolic and organellar ribosomal protein genes did not exhibit the same patterns of expression with respect to the life cycle, with the genes encoding organellar proteins exhibiting more complex expression patterns (i.e. they were assigned to multiple modules; Figure 5B).

The "royalblue" module is another example of a module which did not exhibit marked changes in expression between the gamete and the sporophyte initial cell. This module was highly enriched in genes related to photosynthesis or encoding chloroplast-targeted proteins (Figure 4A,B,C). Based on the transcriptomic data, therefore, both cytosolic translation and photosynthesis appear to be processes that are already important at the gamete stage, although it is possible that transcripts related to these processes may accumulate in gametes but be translated at a later stage.

Comparative analysis of life-cycle-related gene expression between *Ectocarpus* species 7 and *D. dichotoma*

To determine whether the developmental and life-cycle-related transcription patterns observed in *Ectocarpus* species 7 corresponded to common, fundamental features that are shared with other brown algae, a comparative analysis was carried out between *Ectocarpus* species 7 and *D. dichotoma.* These two species are phylogenetically distant within the brown algal tree (Akita *et al.*, 2022). Based on a recent estimate (Choi *et al.*, 2024), their common ancestor dates to about 250

365 Mya. Consequently, if a feature is shared between the two species, this is an indication that it may
366 have been conserved over a significant part of the evolutionary history of the brown algal lineage.
367
368 Replicated transcriptomic data was available for seven stages of the *D. dichotoma* life cycle (Table
369 S1). In a PCA analysis (Figure S10) the adult sporophyte and gametophyte stages clustered together,
370 presumably reflecting the isomorphy between the two generations. Consequently, the distribution of
371 stages in the PCA did not follow the progression of the life cycle, as had been observed for
372 *Ectocarpus* species 7. However, the first dimension clearly separated male gametes from the other *D.*
373 *dichotoma* life cycle stages and the second dimension separated early developmental stages from
374 adult stages. *D. dichotoma* has flagellated male gametes and non-flagellated egg cells. The latter
375 were clustered with early sporophyte stages (zygote and 8h embryo), suggesting that the markedly
376 different gene expression patterns observed in male gametes from the two species compared to
377 other life cycle stages were related to their being actively swimming, flagellated cells rather than
378 being a universal characteristic of all brown algal gametes.
379
380 Life-cycle-related gene expression in *Ectocarpus* species 7 and *D. dichotoma* was compared using two
381 different approaches. The first aimed to determine whether the co-expression patterns of *Ectocarpus*
382 species 7 genes grouped into modules were mirrored by the *D. dichotoma* orthologues of these
383 genes. The second involved independently clustering *D. dichotoma* genes into co-expression modules
384 using life cycle transcriptomic data and then determining whether there were similarities between
385 the modules established for the two species.
386
387 To optimally identify conserved one-to-one orthologues between *Ectocarpus* species 7 and *D.*
388 *dichotoma*, an orthologue analysis was carried out specifically for the two species using Orthofinder
389 (Emms and Kelly, 2019). This approach identified 8,527 one-to-one orthologous relationships
390 between the 18,370 *Ectocarpus* species 7 genes and the 20,583 *D. dichotoma* genes (Table S7). This
391 orthologue dataset was used to compare gene expression patterns in the two species.
392
393 ***D. dichotoma* orthologues of sets of genes from *Ectocarpus* species 7 modules exhibited conserved**
394 **co-expression for some modules that grouped genes involved in the same cellular process**
395
396 To determine whether the co-expression patterns of genes in *Ectocarpus* species 7 modules was
397 conserved in *D. dichotoma,* the *Ectocarpus* species 7 genes in each module were substituted with
398 their *D. dichotoma* orthologues and various parameters, notably the preservation of the density of
399 the module and the preservation of the connectivity, were evaluated (Table S8) using the *D.*
400 *dichotoma* transcriptomic data for the seven different life cycle stages (Table S1). The density
401 preservation of a module was measured by evaluating whether the average correlation for the
402 module was conserved in the second species and whether the module summary profile (module
403 eigengene) still explained a high proportion of the variance after the genes were substituted with
404 orthologues from the second species. Connectivity preservation, on the other hand, determined
405 whether the correlation pattern between the genes was conserved after substitution. Various
406 density and connectivity statistics based on functions in both the WGCNA R package and the NetRep
407 R package were aggregated to estimate conservation of gene co-expression for each *Ectocarpus*
408 species 7 module in *D. dichotoma*.
409
410 Generally, the modules with the best conservation statistics in this analysis were those that had been
411 identified as being highly enriched in *Ectocarpus* species 7 genes with predicted housekeeping
412 functions (Figure 6A). Thus, the “photosynthesis” (“royalblue”), the “ribosome” (“purple”), the
413 “cilium and flagellum” (“turquoise”) and various translation-associated (“greenyellow”, “cyan”, and
414 “magenta”) modules all showed a high level of conservation. The expression pattern of the
415 "darkgreen" module was also considered to be conserved in *D. dichotoma* despite the fact only three
416 orthologues were detected. The "darkgreen" module consists principally of genes located within the

417 non-recombining sex-determining region (SDR) of the female (U) and male (V) sex chromosomes
418 (Ahmed *et al.*, 2014) and is therefore a special case because the co-expression pattern is determined
419 not only by gene expression but also by gene presence (i.e. presence of the U or V sex chromosome
420 in gametophytes). The module was considered to be conserved in *D. dichotoma* because the three
421 orthologues are located in the SDR in both species.
422
423 For modules that had good conservation statistics between the two species, *D. dichotoma*
424 orthologues of the *Ectocarpus* species 7 genes that were best correlated with the module eigengene
425 also exhibited a strong correlation with the module eigengene after the *Ectocarpus* species 7 genes
426 had been replaced with the *D. dichotoma* orthologues (Figure 6B). For example, for the "purple" and
427 "royalblue" modules (which had good conservation statistics; Figure 6A) in the top part of Figure 6B,
428 the *Ectocarpus* species 7 genes that were best correlated with the module eigengene are positioned
429 on the left. In the bottom part of the figure the *D. dichotoma* orthologues of these genes are also
430 positioned on the left and they also show strong correlation with the module eigengene. This
431 conservation of correlation with the module eigengene between orthologues was not observed for
432 modules such as "midnightblue" that had poor conservation statistics between the two species
433 (Figure 6B).
434
435 To summarise, this analysis indicated that the co-expression pattern of the genes in a *Ectocarpus*
436 species 7 module following replacement with the *D. dichotoma* orthologues was only conserved for a
437 subset of the modules. The modules that exhibited conservation of co-expression across the two
438 species in this analysis tended to contain sets of genes that functioned in a basic, evolutionarily-
439 conserved cellular process. Moreover, conservation of module co-expression patterns across the two
440 species appeared to be conferred preferentially by orthologues of the *Ectocarpus* species 7 genes
441 that showed the best correlation with the module eigengene.
442
443 **A subset of life-cycle-related gene co-expression modules were conserved between *Ectocarpus***
444 **species 7 and *D. dichotoma***
445
446 For the second approach to compare life-cycle-regulated gene expression in *Ectocarpus* species 7 and
447 *D. dichotoma,* WGCNA was used to define co-expressed gene modules independently for *D.*
448 *dichotoma* using the replicated transcriptomic data for the seven different *D. dichotoma* life cycle
449 stages (Table S1; Figure S4B). The number of modules defined for *D. dichotoma* was lower than the
450 number that had been obtained for *Ectocarpus* species 7 (nine compared with 23; Figure S10, Tables
451 S6, S9, S10), presumably because data was available for fewer life cycle stages and because the *D.*
452 *dichotoma* adult sporophyte and gametophyte generations are isomorphic and therefore have more
453 similar overall gene expression patterns (Figure S10A). As for the *Ectocarpus* species 7 modules,
454 analysis of enriched GO terms (Figure S11) allowed general biological functions to be manually
455 assigned to a subset of the modules (five of the nine modules; Figure S10A).
456
457 Correlation between modules across the two species was assessed based on the number of shared
458 one-to-one orthologues in pairwise comparisons. Fisher's exact test was used to determine whether
459 *Ectocarpus* species 7 and *D. dichotoma* modules shared a greater number of one-to-one orthologues
460 than expected from a random distribution. This analysis identified several pairs of life-cycle-related
461 gene co-expression modules with significantly conserved gene contents between the two species but
462 not all modules were conserved (Figure 6C). As in the first analysis described above, conservation
463 tended to be strongest for *Ectocarpus* species 7 modules that had been manually assigned general
464 functional annotations and which had registered the highest values for module preservation statistics
465 in the first analysis (Figure 6A).
466
467 "Purple" was one of the most strongly conserved *Ectocarpus* species 7 modules: 131 of its 284 one-
468 to-one orthologues were shared with the *D. dichotoma* "blue" module (Figure 6C), with most of the

469 shared orthologues predicted to encode ribosomal proteins. However, the *D. dichotoma* "blue"
470 module exhibited a marked downregulation in male gametes, which was not observed for the
471 *Ectocarpus* species 7 "purple" module. In contrast, the *Ectocarpus* species 7 "turquoise" module,
472 shared 371 (of a total of 1155) one-to-one orthologues with the *D. dichotoma* "green" module,
473 principally with predicted cilium- and flagellum-related functions (Figure 6C,D), and these two
474 modules also exhibited similar life-cycle-related expression patterns, in particular high levels of
475 expression in male gametes. Therefore, both the gene content and the expression patterns of these
476 two modules appear to have been conserved over evolution. Most of the one-to-one orthologues in
477 the translation-related *Ectocarpus* species 7 modules "cyan", "greenyellow" and "magenta"
478 corresponded with genes in the *D. dichotoma* "turquoise" module, consistent with the poorer
479 resolution of the *D. dichotoma* modules (Figure 6C). Nonetheless, all of these modules exhibited a
480 lower level of gene expression in male gametes, indicating conservation of their expression patterns
481 over evolutionary time.
482
483 Taken together, the comparison between *Ectocarpus* species 7 and *D. dichotoma* indicated that there
484 has been partial conservation of life-cycle-related gene expression patterns between the two species,
485 in particular for modules corresponding to clearly-identifiable cellular functions. Moreover, some
486 modules exhibited conservation not only in terms of gene (orthologue) content but also exhibited
487 similar expression patterns over the course of the life cycle, proving further support for the (partial)
488 conservation of life-cycle-related gene expression patterns over time.
489
490 The above analyses provided no evidence that transcription-related modules were conserved,
491 overall, between *Ectocarpus* species 7 and *D. dichotoma* but a more detailed analysis was carried out
492 to determine whether life-cycle-related expression patterns might have been conserved for
493 individual transcription factor genes. For this, 214 transcription factors with one-to-one orthologues
494 in the two species were selected and their expression patterns (normalized expression z-scores)
495 analysed across six life cycle stages that were approximately equivalent between the two species
496 (gamete, zygote, early sporophyte, adult sporophyte, adult male gametophyte and adult female
497 gametophyte; Figure S12, Table S1). High Pearson correlation coefficients were obtained for a subset
498 of the transcription factors but none of the correlations were significant at $p = 0.05$ after correction
499 for multiple testing (Table S11). However, the applied correction was stringent because a large
500 number of orthologous genes were considered so the most strongly correlated transcription factors
501 may nonetheless merit further study in the future. We noted, for example, that all three members of
502 the TALE homeodomain transcription factor family, which includes the life cycle regulators *ORO* and
503 *SAM* (Arun *et al.*, 2019), were among the genes that exhibited high Pearson correlation coefficients in
504 this analysis (Table S11, Figure 6E).
505
506 **Discussion**
507
508 **Subsets of genes with related functions are co-expressed during the life cycle**
509
510 This study analysed replicated RNA-seq samples for ten different stages of the *Ectocarpus* species 7
511 life cycle to provide an overview of life-cycle-related gene expression in this species. Clustering of
512 genes into co-expression modules indicated that subsets of the genes associated with several cellular
513 processes, including transcription, protein synthesis, flagella biosynthesis/function and
514 photosynthesis, are co-ordinately regulated during the life cycle.
515
516 The coordinated expression patterns of the genes in these modules implies coordinated regulation of
517 transcription and/or mRNA stability over the course of the life cycle. The regulatory systems that
518 mediate this coordinated expression are currently unknown for brown algae but information about
519 the mechanisms that co-ordinately regulate these processes in other eukaryote lineages can provide
520 some indications of possible regulators. For example, in *Ectocarpus* species 7, four different modules

521 were enriched in translation-related genes. In other eukaryotic lineages, a large proportion of
522 ribosomal protein genes are regulated by the mTOR/PKA pathway (Martin *et al.*, 2004; Ni and
523 Buszczak, 2023). Interestingly, genes predicted to encode cytosolic and organellar ribosomal proteins
524 were regulated differently in *Ectocarpus* species 7. Note also that this conservation of expression
525 patterns provides additional support for the transfer of the *Arabidopsis* ribosomal protein gene
526 nomenclature (Scarpin *et al.*, 2023) to *Ectocarpus* species 7 genes
527 (https://bioinformatics.psb.ugent.be/orcae/overview/EctsiV2) based on sequence similarity.
528
529 In land plants, photosynthesis-related genes have been shown to be regulated by both light and
530 developmental cues and the regulatory pathways have been characterised. Phytochrome signalling
531 counteracts negative regulation of photosynthesis genes by transcription factors such as
532 PHYTOCHROME-INTERACTING FACTOR (PIF), PIF-LIKE (PIL) and GOLDEN2-LIKE1 (GLK1), which act
533 downstream of various developmentally regulated pathways (Waters *et al.*, 2009; Wang *et al.*, 2017).
534 However, orthologues of these transcription factors have not been found in brown algae and,
535 consequently, coordinated regulation of photosynthetic genes in brown algae, as was observed here
536 for the "royalblue" module, presumably involves a different set of actors.
537
538 As far as flagella- and cilium-related genes are concerned, these organelles are widespread in
539 eukaryotes and the last eukaryotic common ancestor (LECA) probably possessed cilium-related
540 structures (Carvalho-Santos *et al.*, 2011). In Metazoans, two transcription factor families, FOXJ1 and
541 RFX, control the formation of core components of all types of cilia (Choksi *et al.*, 2014). However,
542 although *Saccharomyces cerevisiae* also possesses an *RFX* gene, this family of transcription factors
543 has only been shown to regulate ciliogenesis in metazoans and is not found outside the opisthokonts
544 (Chu *et al.*, 2010). In *Chlamydomonas reinhardtii*, ciliogenesis is under the control of XAP5 (Li *et al.*,
545 2018), a transcription factor that is widely distributed across eukaryotic lineages. Neither *FOXJ1* nor
546 *RFX* have been found in brown algal genomes, but *Ectocarpus* species 7 does possess an *XAP5*
547 homologue (LocusID Ec-05_002220). This gene therefore represents a possible candidate for future
548 analysis of the regulation of this pathway.
549
550 These examples illustrate how candidate regulatory genes may be identifiable for cellular processes
551 that are highly conserved across eukaryotes but candidates are more difficult to identify for modules
552 that group brown-algal-specific genes of unknown function or functions such as the PL41 and GT23
553 gene families that do not have equivalents in other eukaryotic lineages. In some instances, regulatory
554 genes may show similar expression patterns to the genes they regulate as a result of auto-regulation,
555 and therefore be included within a co-expression module, but this will not be the case for all
556 regulators.
557
558 **Identification of marked transcriptome changes during early sporophyte development**
559
560 Analysis of RNA-seq data for multiple developmental stages of *Ectocarpus* species 7 provided a broad
561 overview of gene expression throughout the life cycle, with a particular focus on the early stages of
562 sporophyte development. Progression through the life cycle was correlated with concomitant,
563 progressive changes in the composition of the transcriptome (Figure 3A) and a particularly marked
564 change in composition occurred at the transition from the gamete stage to the initial stage of
565 sporophyte development. Most of the gene co-expression modules identified in this study exhibited
566 changes in transcript abundance at this transition and more than half of the genes in the genome
567 were differentially expressed between the two stages.
568
569 Periods of large-scale changes in transcriptome composition have been observed during early
570 development of both animals and land plants (Xue *et al.*, 2013; Anderson *et al.*, 2017; Vastenhouw *et*
571 *al.*, 2019; Zhao *et al.*, 2019), where they tend to coincide with the maternal-to-zygotic transition
572 (MZT). The MZT corresponds to the switch from reliance on maternal transcripts supplied to the

transcriptionally-inactive egg cell to mRNAs produced by transcription of the zygote genome (Tadros and Lipshitz, 2009; Vastenhouw *et al.*, 2019). During the MZT, induction of the expression of genes in the zygote genome, which is referred to as zygotic gene activation (ZGA), coincides with a phase of degradation of maternal transcripts in both animals and land plants. The exact timing of MZT varies across species, occurring rapidly in land plants, only hours after zygote formation (Anderson *et al.*, 2017; Chen *et al.*, 2017; Zhao *et al.*, 2019), but considerably later in animals, for example occurring three days after fertilisation in 8-cell human embryos (Xue *et al.*, 2013). However, even in animals, 1-cell stage embryos exhibit a distinct transcriptome pattern (Xue *et al.*, 2013).

Ectocarpus is not oogamous and both male and female gametes are small, flagellated cells that swim actively for a significant part of their lifetime. It therefore seems likely that these cells are already transcriptionally active during the gamete stage, in which case they would not rely solely on maternally-produced transcripts (although this has not yet been investigated experimentally). Consequently, it is not clear whether there is a specific phase of degradation of maternal transcripts in gametes equivalent to the phases of maternal transcript degradation that have been observed at the MZT in land plants and animals. However, the marked change in transcriptome composition during early development is a feature that is shared with animals and land plants, underlining the broad importance of large-scale transcriptional changes during early development.

In terms of functional categories, fewer genes involved in flagellar function or transcription were expressed after the transition from the gamete stage to the initial stage of sporophyte development. Downregulation of flagellar genes is expected for this transition from a flagellated to a non-flagellated cell. The reduction in the number of expressed transcription factor genes is more surprising but it is likely that the nature of the transcription factor genes expressed or repressed at this stage is more important than the overall number of transcription factor genes expressed. Trends in transcription factor gene up- and down-regulation are not consistent across species, with a decrease in the number of different transcription factor gene transcripts observed in *Arabidopsis* (Zhao *et al.*, 2019) but an increase in rice (Anderson *et al.*, 2017), maize (Chen *et al.*, 2017) and human (Xue *et al.*, 2013), coinciding with the MZT. Moreover, in rice and maize, specific loci that play key roles during embryogenesis such as members of the BABYBOOM and WUSCHEL gene families are upregulated at the MZT/ZGA, supporting the idea that the identity of the specific transcription factor genes expressed is more important than the overall numbers (Anderson *et al.*, 2017; Chen *et al.*, 2017). Note that *Ectocarpus* has AP2 domain and homeodomain proteins but no close homologues of the BABYBOOM and WUSCHEL families so it is likely that different transcriptional regulators are involved in regulating development at the equivalent stage in brown algae.

Analysis of modules that exhibited overall gene upregulation between the gamete and early sporophyte stages identified translation as a general function that was upregulated during this transition. However, the upregulation of these genes does not appear to have corresponded to *de novo* induction of translation because a subset of translation-related genes was already expressed at the gamete stage. The overall gene expression pattern is more indicative of a step increase in translation capacity or complexity in the early sporophyte compared to the gamete.

Conservation of life-cycle-related gene expression patterns across brown algal species

Comparison of generation-biased gene expression between adult gametophyte and sporophyte stages across ten brown algal species identified a strong positive correlation between the degree of dimorphism between generations and the number of GBGs identified per species, indicating that the majority of GBG expression is related directly or indirectly to thallus morphology, at least for the adult stages analysed. Orthologue analysis indicated only weak overlap between GBG sets from different species, supporting an earlier conclusion that there is rapid turnover of GBG sets in brown algae (Lipinska *et al.*, 2019). Interestingly, however, analysis of GO enrichment in GBG sets indicated

625 that several broad functional categories were conserved across gametophyte-biased gene sets,
626 whereas different broad functional categories were conserved across sporophyte-biased gene sets
627 (Figure 2). This observation suggests that the two generations have conserved life-cycle-related
628 functional characteristics that are independent of morphological complexity or the degree of
629 dimorphism between generations.
630
631 The analysis of whole adult individuals to study GBG expression therefore identified some interesting
632 conserved life-cycle-related features but the resolution of this approach is limited because only one
633 sporophyte stage and one gametophyte stage was analysed per species and because, at the adult
634 stage, the data represent an average view of the transcriptomes of multiple different cell types. The
635 comparative analysis of multiple stages of early sporophyte development in *Ectocarpus* species 7 and
636 *D. dichotoma* allowed a more detailed analysis of developmentally regulated gene expression and,
637 notably, showed that there was considerable conservation of co-expressed gene modules between
638 two species, particularly for modules that were enriched in genes involved in evolutionarily-
639 conserved functional categories. Moreover, when the known life cycle regulatory genes *SAM* was
640 analysed, there was clear evidence of conservation of its expression patterns across the two species.
641 These results underline the importance of carrying out detailed transcriptomic analyses to identify
642 and investigate conserved life cycle regulatory pathways.
643
644 **Materials and Methods**
645
646 **Life cycle stages and variants on the sexual cycle**
647
648 Both *Ectocarpus* species 7 and *D. dichotoma* have haploid-diploid life cycles that involve alternation
649 between a sporophyte and a gametophyte generation (Müller, 1967; van den Hoek *et al.*, 1995).
650 During the sexual life cycle, the diploid sporophyte generation produces haploid meio-spores through
651 meiosis. These spores germinate into haploid gametophytes that can be male or female (dioicy).
652 Male and female gametes, produced, respectively, by male and female gametophytes, fuse to
653 produce a diploid zygote, which, in turn, develops into the next sporophyte generation. In *Ectocarpus*
654 species 7, the germinating zygote undergoes a developmentally symmetrical first division to produce
655 a basal filament, which then branches to establish a basal filament system consisting of round and
656 elongated cells. Once this basal system is established, upright filaments consisting of cylindrical cells
657 grow up into the medium and these filaments bear the sexual structures, plurilocular sporangia and
658 unilocular sporangia (Peters *et al.*, 2008). *Ectocarpus* species 7 also exhibits variations on this basic
659 sexual life cycle, at least in culture (Müller, 1967). For example, parthenogenesis of unfertilised
660 gametes gives rise to haploid partheno-sporophytes. A few hours after release from the plurilocular
661 sporangia, unfertilized free-swimming male gametes attach to the substrate, loose their flagella and
662 acquire a round shape. Upon attachment they start to develop a cell wall. After about two days, the
663 initial cell elongates and divides, producing the first cells of the sporophytic basal filaments. All but
664 one of the sporophyte stages analysed in this study corresponded to partheno-sporophyte samples.
665 Partheno-sporophytes exhibit identical morphology and reproductive functionality to diploid
666 sporophytes and pure samples of early-stage diploid sporophytes are difficult to obtain because of a
667 high level of gamete parthenogenesis in genetic crosses (Coelho *et al.*, 2012a).
668
669 **Publicly available RNA-seq datasets**
670
671 RNA-seq data for the sporophyte and gametophyte generations of the following ten species was
672 recovered from the Phaeoexplorer website (https://phaeoexplorer.sb-roscoff.fr/) or from public
673 databases: *Macrocystis pyrifera, Saccharina latissima, Saccharina japonica, Saccorhiza polyschides,*
674 *Myriotrichia claveaformis, Pylaiella littoralis, D. dichotoma, Sphacelaria rigidula, Ectocarpus* species 7
675 and *Scytosiphon promiscuus*. In addition, RNA-seq data was collected for multiple stages of the *D.*

676 *dichotoma* and *Ectocarpus* species 7 life cycles. All the accession numbers for these data are listed in
677 Table S1.
678
679 **Comparisons of orthologues across multiple brown algal species**
680
681 To compare orthologues across the ten brown algal species analysed for generation-biased gene
682 expression an orthogroup analysis was carried out using Orthofinder (Emms and Kelly, 2019) version
683 2.5.2. Strict selection of only one-to one orthologues did not identify sufficient orthologues (1,038),
684 principally due to gene model fragmentation in the lower quality genome assemblies. A more relaxed
685 selection approach was therefore used, taking into account genome assembly quality. This relaxed
686 approach, which required exactly one orthologue from the best quality assemblies (*D. dichotoma*,
687 *Ectocarpus* species 7, *P. littoralis*, *S. latissima*, *S. promiscuus* and *S. rigidula*), between zero and two
688 orthologues for *M. pyrifera*, zero or one orthologue for *S. japonica*, and any number of orthologues
689 for *S. polyschides* and *M. clavaeformis*, identified 9,317 orthogroups (Table S3). The assumption
690 underlying this approach was that the multiple gene models in the poor-quality genomes
691 corresponded to fragments of a single gene but note that we cannot rule out the possibility that a
692 minority of these groups of genes corresponded to tandem gene duplications. To calculate
693 generation bias when a species possessed more than one gene model in a particular orthogroup,
694 each model was given a score of +1, -1 or 0 if the expression data indicated that they were
695 sporophyte-biased/specific, gametophyte-biased/specific or neither, respectively. The mean of these
696 values was then calculated and the orthologue was classed as sporophyte-biased, gametophyte-
697 biased or unbiased if the value was >0, <0 or 0, respectively.
698
699 **Algal strains and culture conditions**
700
701 *Ectocarpus* species 7 strain Ec32 gametophytes were grown in sterile Provasoli-enriched (0.5x)
702 natural sea water at 13°C under 12h:12h day:night conditions until they reached maturity.
703 Synchronous gamete release was induced by removing excess seawater and incubating in the dark
704 and in the cold for 1 h. Sterile Provasoli-enriched (0.5x) natural sea water (Starr and Zeikus, 1993;
705 Coelho *et al.*, 2012b) was then added and the gametophytes incubated for 30 min to allow gamete
706 release. The medium was filtered through 1 µm cell strainer (pluriSelect, Leipzig, Germany) to
707 eliminate any contaminating gametophytic fragments. The gamete suspension was then diluted to a
708 concentration of 1.5 million cells per mL (A_{450nm} = 0.01) to produce a density of 300 cells per mm² on
709 plastic 150 cm Petri dishes after gamete settlement. After gamete release, the Petri dishes were
710 incubated at 13°C under 12h:12h day:night conditions at a light intensity of 40 $\mu mol.m^{-2}.s^{-1}$ for 24 or
711 48 h. Cultures were sampled in the late afternoon to ensure homogeneity with regard to circadian
712 rhythms. Sampling was carried out by scraping the bottom of the culture plate with a cell scraper
713 (Sarstedt, Nümbrecht, Germany) after the seawater medium had been removed. The cell suspension
714 was centrifuged at 14000 g for 15 min and the pellet flash-frozen in liquid nitrogen.
715
716 **RNA extraction and RNA-seq sequencing and mapping**
717
718 RNA was extracted using the Macherey Nagel Nucleospin Plant and Fungi kit (Hoerdt, France). Frozen
719 pellets were resuspended in lysis buffer (500 µL of PFL buffer, 40 µL of PFR buffer and 50 µL of 1 M
720 DDT per sample) and the cells were lysed by three 30-second treatments at 7800 rpm in 2 mL "tough
721 micro-organism" lysis tubes (VK05) in a Precellys Evolution homogeniser (Bertin Technologies,
722 Montigny-le-Bretonneux, France), followed by a 5 min incubation at 56°C. RNA extraction followed
723 the manufacturer's instructions except that a DNA digestion step was added after the first wash
724 (digestion on the column with 5 µL of Qiagen DNAse I in 75 µL RDD buffer for 20 s before a second
725 wash with PFW I buffer). The PFW II buffer wash step was carried out three times. RNA was eluted in
726 50 µL of RNAse-free H_2O. RNA-seq libraries were constructed after oligo-dT selection and sequenced
727 by Genewiz (Leipzig, Germany) on an Illumina NovaSeq 6000, using a standard unstranded paired-

end protocol to produce a minimum of 50 million reads per condition. Data quality was assessed with FastQC (Andrews, 2016) version 0.11.0 or 0.11.9 and reads were trimmed with Trim Galore (Krueger, 2015) version 0.6.5 with parameters --illumina --length 50 --quality 24 --stringency 6 --max_n 3. Genomes were indexed and data was mapped onto the v2 version of the *Ectocarpus* species 7 reference genome (Sterck *et al.*, 2012; Cormier *et al.*, 2017) using HISAT2 (Kim *et al.*, 2019) version 2.1.0 with default parameters (the parameter --rna-strandedness was specified according to the information in Table S1). The output was converted to bam format and ordered and indexed using the SAMtools (Danecek *et al.*, 2021) version 1.10 functions order and index. Quantification of transcript abundance was carried out using the featureCounts function (Liao *et al.*, 2014) from the Subread package version 2.0.1 on CDS features grouped by Parent or LocusID.

Identification of differentially expressed genes

Differentially expressed genes were identified using DESeq2 (Love *et al.*, 2014) version 1.34.0 in R version 4.1.2. Genes were considered to be differentially expressed if they had an adjusted (Benjamini-Hochberg false discovery rate) *p*-value of <0.05 and an absolute $\log_2$(FoldChange) greater than 1. Breakpoints in gene expression trends were analysed using the Trendy R package (Bacher *et al.*, 2018) version 1.16.0 with the functions trendy (maxK = 3, pvalCut = 0.05) and topTrendy (adjR2Cut = 0.5). DESeq2 version 1.34.0 was also used to calculate normalised counts (NormalisedCounts) using the median of ratios method. Transcripts per kilobase million (TPM) values were calculated from counts of mapped reads using an in-house custom script. Based on the differential expression analyses and the TPM values, genes were classified into six categories: gametophyte-biased (mean gametophyte and mean sporophyte TPM values both ≥1, log2(fold change) ≥1, adjusted *p*-value <0.05), sporophyte-biased (mean gametophyte and mean sporophyte TPM values both ≥1, log2(fold change) ≤-1, adjusted *p*-value <0.05), gametophyte-specific (mean TPM < 1 for the sporophyte and ≥1 for the gametophyte, log2(fold change) ≥1, adjusted *p*-value <0.05), sporophyte-specific (mean TPM <1 for the gametophyte and ≥1 for the sporophyte, log2(fold change) ≤-1, adjusted *p*-value <0.05), unbiased genes (mean gametophyte and mean sporophyte TPM values ≥ 1, log2(fold change) <1 or >-1 and/or adjusted *p*-value ≥ 0.05) and unexpressed genes (mean gametophyte and mean sporophyte TPM values both <1).

Gene ontology and prediction of subcellular localisation

Gene ontology term annotations were extracted from the Interproscan annotation files generated by the Phaeoexplorer consortium (https://phaeoexplorer.sb-roscoff.fr/downloads/; Denoeud *et al.*, 2024). The subcellular localisation of proteins was predicted by identifying amino-terminal targeting peptides using HECTAR version 1.3 (Gschloessl *et al.*, 2008).

Calculation of breadth of expression and Jaccard indices

Breadth of expression (tau) was calculated using a custom script in R based on the following formula:

$$\tau = (\Sigma(1 - \hat{x}_i))/(n-1)$$

where $\hat{x}_i$ is the expression level of gene i normalized by the maximum expression value across all conditions (mean $\log_2$(NormalisedCounts +1)), and n is the number of conditions.

Jaccard indices were calculated and plotted using vegan version 2.6.8 (https://cran.r-project.org/web/packages/vegan/index.html).

Enrichment analysis

Enrichment of co-expression modules in differentially-expressed genes, predicted subcellular localisations or gene ontology terms were computed using the enricher function from the R package

780 clusterProfiler (Yu *et al.*, 2012) version 4.2.2. *p*-values were adjusted for multiple testing based on
781 the Benjamini-Hochberg false discovery rate.
782
783 **Identification of modules of co-expressed genes**
784
785 For both the *Ectocarpus* species 7 and the *D. dichotoma* datasets, raw counts were normalised using
786 the estimateSizeFactors and counts (with option normalized = TRUE) functions from the R package
787 DESeq2 (Love *et al.*, 2014) version 1.34.0. Genes with a normalised count below 45 in all the samples
788 analysed for the relevant species were removed. The normalised counts matrix was then
789 transformed with the log1p (=$\log_2(x+1)$) R function. To fit a scale-free topology model, the soft-
790 thresholding power was selected using the pickSoftThreshold function, and gene modules were built
791 using the blockwiseModules function from the WGCNA R package (Langfelder and Horvath, 2008)
792 version 1.71. For *Ectocarpus* species 7, this function was run with options power = 16, maxBlockSize =
793 16100 (which yields a topological matrix in one block), minModuleSize = 30, reassignThreshold = 0,
794 mergeCutHeight = 0.2, pamRespectsDendro = FALSE, randomSeed = T, corType = "Pearson". For *D.*
795 *dichotoma,* the function was run with power = 18, maxBlockSize = 16000 (which yields a topological
796 matrix in one block), minModuleSize = 30, reassignThreshold = 0, mergeCutHeight = 0.25,
797 pamRespectsDendro = FALSE, randomSeed = T, corType = "Pearson". Complete module annotation
798 and module membership (MM) scores (or kME, representing the correlation between the gene and
799 the module eigengene) can be found, together with associated *p*-values, in Supplementary Tables S6
800 and S8. *D. dichotoma* gene module descriptions are in Figure S10B.
801
802 **Conservation of gene co-expression modules between *Ectocarpus* species 7 and *D. dichotoma***
803
804 An orthologue analysis was carried out specifically for *Ectocarpus* species 7 and *D. dichotoma* using
805 Orthofinder (Emms and Kelly, 2019) version 2.5.2 to optimise the identification of one-to-one
806 orthologues for these two species (Table S7). The one-to-one orthologue set generated by this
807 analysis was then used to evaluate module conservation across the two species. The WGCNA
808 package modulePreservation function (networkType = "signed", nPermutations = 20,
809 maxGoldModuleSize = 1000, maxModuleSize = 2500) and the NetRep package (Ritchie *et al.*, 2016)
810 version 1.2.7 modulePreservation function (nPerm=10000, on the WGCNA-computed correlation and
811 TOM matrices) were used to compute module preservation statistics. In addition, the silhouette
812 coefficient for modules was computed using the silhouette_SimilarityMatrix function from the
813 CancerSubtypes R package (Xu *et al.*, 2017) version 1.20.0 on the correlation matrix. All values can be
814 found in Table S8. The gene correlation heatmap (Figure 6B) was produced using the NetRep (Ritchie
815 *et al.*, 2016) version 1.2.7 plotCorrelation function. The gold module was a random sample of 1,000
816 *Ectocarpus* species 7 genes that provided a control distribution of gene expression patterns for
817 comparisons with *D. dichotoma* modules. Cross-species module comparisons were visualized as a
818 contingency table (Figure 6C) constructed by interpolating orthologous gene counts between the
819 *Ectocarpus* species 7 and *D. dichotoma* datasets. For each pair of modules, a list of orthologues
820 present in at least one of the two modules was established and a Fisher's exact test was performed
821 on Boolean vectors indicating whether each gene was present in each of the two modules to assess
822 the statistical association between module assignment in both species. The objective was therefore
823 to determine whether each pair of *Ectocarpus* species 7 and *D. dichotoma* modules shared a greater
824 number of one-to-one orthologues than expected from a random distribution. Fisher's exact test was
825 applied using the fisher.test function from the R stats package (version 4.1.2). Cells in the
826 contingency table were colour-coded according to $-\log_{10}$(*p*-value).
827
828 The contingency table (Figure 6C) was constructed by interpolating gene counts between the
829 *Ectocarpus* species 7 and *D. dichotoma* datasets and using the fisher.test function (alternative =
830 "greater") from the R stats package (version 4.1.2).
831

832 **Detection of conservation of gene expression patterns between *Ectocarpus* species 7 and *D.***
833 ***dichotoma***
834
835 To assess gene expression pattern preservation between *Ectocarpus* species 7 and *D. dichotoma,* a z-
836 score (mean for one condition – mean across all conditions) / standard deviation) was computed
837 from the $\log_2$(NormalisedCounts+1) values for each of the six common timepoints between the
838 *Ectocarpus* species 7 and *D. dichotoma* datasets (Table S1). A Pearson correlation coefficient was
839 then calculated using the R stats package (version 4.1.2) cor.test function (alternative = "greater",
840 method = "pearson").
841
842 **Manual reannotation of ribosomal protein genes and three-dimensional representation of**
843 **ribosomal proteins**
844
845 *Ectocarpus* species 7 ribosomal proteins were manually annotated using the recent *Arabidopsis*
846 *thaliana* nomenclature (Scarpin *et al.*, 2023) as a reference (Table S12). *Ectocarpus* species 7
847 ribosomal proteins were compared with the *A. thaliana* ribosomal protein dataset using BLASTp and
848 the annotations transferred based on the best BLASTp match. To visualise differentially expression in
849 relation to the structure of the ribosome, *Ectocarpus* species 7 ribosomal proteins were mapped
850 onto the *Triticum aestivum* ribosome structure (Protein data bank model 4V7E; Gogala *et al.*, 2014)
851 and the mapping was visualised using UCSF ChimeraX version 1.9 (Meng *et al.*, 2023).
852
853 **General data treatment and figure preparation tools**
854
855 Several R modules were used at multiple stages of the study. These included rtracklayer (Lawrence *et*
856 *al.*, 2009) version 1.52.1, Tidyverse (Wickham *et al.*, 2019) version 2.0.0, and sjmisc (Lüdecke, 2018)
857 version 2.8.9, which were used to handle and analyse data, and ggplot2 (Wickham *et al.*, 2016)
858 version 3.4.2 and Pheatmap (Kolde, 2019) version 1.0.12, which were used to generate figures.
859
860 **Data availability**
861
862 All the new sequence data generated by this study have been deposited in the European
863 Bioinformatics Institute/European Nucleotide Archive (EBI/ENA) database and are publicly available
864 (see Table S1 for details).
865
866 **CRediT authorship contribution statement**
867
868 Conceptualization: P.R., O.G., J.M.C.; Formal analysis: P.R., O.G.; Investigation: P.R., O.G.; Resources:
869 B.N., J.-M.A; Data Curation: P.R., O.G.; Writing - Original Draft: P.R.; Writing - Review & Editing: all
870 authors; Visualization: P.R., O.G.; Supervision: O.G., J.M.C.; Project administration: J.M.C.; Funding
871 acquisition: : J.M.C.
872
873 **Declaration of competing interest**
874
875 The authors declare that they have no known competing financial interests or personal relationships
876 that could have influenced the work reported in this paper.
877
878 **Funding**
879
880 This work was supported by the ANR project Epicycle (ANR-19-CE20-0028-01), the France
881 Génomique National infrastructure project Phaeoexplorer (ANR-10-INBS-09), the CNRS and Sorbonne
882 University.
883

Acknowledgments

We would like to thank Julia Morales for helpful discussions about ribosomal proteins, Laurence Dartevelle and Elodie Rolland for help with algal cultures, Delphine Scornet, Masakazu Hoshino, Inka Bartsch, Akira F. Peters, Samuel Boscq, Shannon DeVanney for providing seaweed photographs. We are grateful to the Roscoff Bioinformatics platform ABiMS (http://abims.sb-roscoff.fr), which is part of the Institut Français de Bioinformatique (ANR-11-INBS-0013) and BioGenouest network, for providing both help and computing and storage resources.

Figures

Figure 1. Generation-biased gene expression across the brown algae

A. Cladogram of the brown algae showing the ten species for which generation-biased gene expression was compared. Adapted from (Cock *et al.*, 2014). **B.** Generation-biased gene expression in relation to life cycle dimorphism. Pie diagrams indicating the proportions of sporophyte-specific (dark red), sporophyte-biased (light red), gametophyte-specific (dark blue), gametophyte-biased (light blue) and unbiased (grey) genes in species with different haploid-diploid life cycles ranging from sporophyte-dominant through isomorphic to gametophyte-dominant (indicated by the red and blue wedges). sp., species. **C.** Overlaps (Jaccard index) between sets of gametophyte-biased/specific and sporophyte-biased/specific genes across the ten species.

Figure 2. Biological function gene ontology term enrichment in the generation-biased/specific gene sets of the ten species

Conserved general functional categories are indicated by coloured boxes. padj, *p*-value adjusted for multiple testing based on the Benjamini-Hochberg false discovery rate.; GA, gametophyte; SP, sporophyte.

Figure 3. Gene expression patterns during the *Ectocarpus* species 7 life cycle

A. Principal component analysis of the *Ectocarpus* species 7 gene expression across ten life cycle stages. The numbers in circles refer to the differential gene expression analyses illustrated in C and D. **B.** Percentage changes in gene expression (regression breakpoints) during *Ectocarpus* species 7 sporophyte development (from left to right, transitions between free-swimming male gamete, sporophyte initial cell (24 hours after gamete release), elongating sporophyte initial cell (48 hours after gamete release), sporophyte 2-5 cell stage, non-fertile adult sporophyte and fertile sporophyte). **C.** Proportions of differentially expressed genes in the transitions between 1) free-swimming male gamete and sporophyte initial cell stage, and 2) adult sporophyte and gametophyte stages, determined using DESeq2 (Table S1). **D.** Density distribution of the $|\log_2(\text{FoldChange})|$ for upregulated and downregulated genes in the differential gene expression analysis described in C. Dotted lines indicate mean values.

Figure 4. Characterisation of gene co-expression modules in *Ectocarpus* species 7

A. Functional categories manually assigned to modules based on Gene Ontology term enrichment analysis of each module. **B.** Enrichments in sub-cellular localisations based on HECTAR predictions: mitochondria (small ellipses), plastid (tube shape with thylakoids) and signal peptide/anchor peptide for secreted proteins. Note that HECTAR does not predict nuclear localisation. **C.** Proportion of differentially expressed genes (DESeq2 adjusted *p*-value < 0.05 and |log2FoldChange| > 1) in each gene module in the transitions between 1) free-swimming male gametes and sporophyte initial cell stage, and 2) adult sporophyte and gametophyte (Table S1). Significant enrichment (indicated by a darker shade of green or orange) means that the proportion of differentially expressed genes in the module was significantly greater (ClusterProfiler adjusted *p*-value < 0.05) than the proportion for the entire genome. **D.** Average module gene expression profile computed on genes with a WGCNA module MM > 0.86 for, from left to right: free-swimming male gamete, sporophyte initial cell (24

936 hours after gamete release), elongating sporophyte initial cell (48 hours after gamete release),
937 sporophyte 2-5 cell stage, non-fertile adult sporophyte, fertile sporophyte, non-fertile female and
938 male gametophytes, fertile female and male gametophytes developmental stages. **E.** Number of
939 genes in the module positively or negatively correlated with the module eigengene. **F.** Module
940 eigengene dendrogram showing the relationship between module eigengenes.
941
942 **Figure 5. Expression of translation-related genes during *Ectocarpus* species 7 development**
943 **A.** Mean expression profile computed for genes with a WGCNA module MM > 0.86 for (from left to
944 right): free-swimming male gamete, sporophyte initial cell (24 hours after gamete release),
945 elongating sporophyte initial cell (48 hours after gamete release), sporophyte 2-5 cell stage, non-
946 fertile adult sporophyte, fertile sporophyte, non-fertile female and male gametophyte, fertile female
947 and male gametophyte developmental stages in modules "purple", "cyan", "greenyellow",
948 "magenta". **B and C.** Heatmaps showing $\log_2$(NormalisedCounts+1) values across the same
949 developmental timepoints as in **A** for manually reannotated ribosomal protein genes corresponding
950 to cytosolic, chloroplast and mitochondrial ribosomal subunits (**B**) and translation-related genes (**C**).
951 Left annotation track: differential expression analysis results for the transitions between 1) free-
952 swimming male gamete and sporophyte initial cell stage, and 2) adult sporophyte and adult
953 gametophyte; right annotation track: WGCNA module colours. **D.** Schematic representation of
954 translation-related functions enriched in the "greenyellow", "purple", "magenta", "cyan" modules.
955 When it was possible to manually assign a general function to a module, the annotation is indicated
956 in brackets after the module name. **E.** Gene ontology terms significantly enriched in the sets of genes
957 clustered within the "purple", "greenyellow", "cyan", and "magenta" modules in *Ectocarpus* species
958 7. Enrichment is indicated as log2 of the ratio of the proportion of genes assigned to the GO term in
959 the module divided by the proportion for the whole genome. CC, cellular component; BP, biological
960 process; MF, molecular function.
961
962 **Figure 6. Conservation of life-cycle-related gene co-expression patterns between *Ectocarpus***
963 **species 7 and *D. dichotoma***
964 **A.** WGCNA density and connectivity median rank statistics indicating the degree of conservation of
965 gene co-expression patterns when of *Ectocarpus* species 7 genes in *Ectocarpus* species 7 co-
966 expression modules were substituted with their *D. dichotoma* orthologues. Manually-assigned
967 general biological functions are indicated in boxes. SDR, sex-determining region. Module size
968 indicates the number of one-to-one orthologues in each module. The modules "darkred" and
969 "darkturquoise" were not included in this analysis because they had only one and zero orthologues,
970 respectively (Table S6). TF, transcription factor; SDR, sex-determining region. **B.** Correlation heatmap
971 comparing three *Ectocarpus* species 7 modules between *Ectocarpus* species 7 and *D. dichotoma*:
972 "midnightblue" (very poor conservation), "purple", and "royalblue" (good conservation). The lower
973 half of the heatmap was calculated based on the expression pattern of the *D. dichotoma* orthologue
974 of each *Ectocarpus* species 7 gene in each module. **C.** Counts of shared one-to-one orthologues
975 between gene co-expression modules defined for *Ectocarpus* species 7 (x-axis) and *D. dichotoma* (y-
976 axis). The colour code represents the $\log_{10}$(*p*-value) for Fisher's exact test (red bar), which was
977 applied to determine whether pairs of modules shared a greater number of one-to-one orthologues
978 than expected from a random distribution. Numbers after the module names indicate the number of
979 one-to-one orthologues in each module. The "darkturquoise" module was not included in this
980 analysis because it contained zero orthologues (Table S6) **D.** Heatmap showing the expression levels
981 ($\log_2$(NormalisedCounts+1)) of 20 selected one-to-one orthologous flagellum-related genes in
982 *Ectocarpus* species 7 and *D. dichotoma*. *Ectocarpus* species 7 timepoints: free-swimming male
983 gamete, sporophyte initial cell (24 hours after gamete release), elongating sporophyte initial cell (48
984 hours after gamete release), sporophyte 2-5 cell stage, non-fertile adult sporophyte, fertile
985 sporophyte, non-fertile female and male gametophytes, fertile female and male gametophytes. *D.*
986 *dichotoma* timepoints: sperm, egg cell, zygote, embryo, adult non-fertile sporophytes, and female
987 and male gametophytes. **E.** Computed z-score based on $\log_2$(NormalisedCounts+1) values for three

988 TALE homeodomain transcription factors over six developmental stages shared between *Ectocarpus*
989 species 7 and *D. dichotoma*, namely sperm, zygote, early sporophyte, non-fertile sporophyte, female
990 and male gametophyte. The Pearson correlation coefficient between the two expression datasets
991 (cor) and the associated *p*-value are indicated.
992
993 **Supplementary Data**
994
995 **Figure S1. Schematic life cycles and photographs of the sporophyte and gametophyte generations**
996 **of brown algal species analysed in this study illustrating the different degrees of generational**
997 **dimorphism.**
998 The life cycle and the morphology and size of the sporophyte and gametophyte generations of
999 *Saccharina japonica* (not shown) are highly similar to those of *Saccharina latissima*. Photograph
1000 credits: *M. pyrifera* sporophyte, Shannon DeVanney; *S. latissima*, Samuel Boscq; *M. clavaeformis*,
1001 Akira F. Peters (Bezhin Rosco); *S. promiscuus* sporophyte, Masakazu Hoshino (note that this
1002 photograph actually shows a sporophyte of *Scytosiphon shibazakiorum*, which is a cryptic species
1003 with identical morphology to *S. promiscuus;* Hoshino and Kogame, 2019); *P. littoralis* gametophyte,
1004 Inka Bartsch (Alfred Wegener Institut) and Delphine Scornet (Roscoff Biological Station); *P. littoralis*
1005 sporophyte, Alfred Wegener Institut and Delphine Scornet (Roscoff Biological Station); *S. polyschides*
1006 gametophyte, *M. pyrifera* gametophyte, *E. siliculosus*, Delphine Scornet (Roscoff Biological Station).
1007
1008 **Figure S2. Light microscopy images of *Ectocarpus* species 7 initial cell and elongating initial cell**
1009 **A.** *Ectocarpus* species 7 strain Ec32 initial cell (settled male Ec32 gamete, 24 h after release). **B.**
1010 *Ectocarpus* species 7 strain Ec32 elongating initial cell (settled male gamete, 48 h after release).
1011 Inverted Leica microscope, magnification: x200, scale bar: 100 µm.
1012
1013 **Figure S3. Breadth of expression (tau) of genes that were differentially expressed, or not, across**
1014 **the transition from gamete to sporophyte initial cell.**
1015 Significantly downregulated and upregulated genes were identified using DESeq2. Dotted lines
1016 indicate mean tau values.
1017
1018 **Figure S4. Hierarchical cluster trees showing co-expression modules identified using WGCNA.**
1019 **A.** *Ectocarpus* species 7. **B.** *D. dichotoma.* Grouped branches correspond to modules, which are
1020 indicated by coloured boxes underneath the tree.
1021
1022 **Figure S5. Enriched GO terms in *Ectocarpus* species 7 gene modules**
1023 Statistically-significant enriched GO terms in *Ectocarpus* species 7 gene modules. Enrichment is
1024 indicated as log2 of the ratio of the proportion of genes assigned to the GO term in the module
1025 divided by the proportion for the whole genome. When it was possible to manually assign a general
1026 function to a module, the annotation is indicated in brackets after the module name. padj, *p*-value
1027 adjusted for multiple testing based on the Benjamini-Hochberg false discovery rate.
1028
1029 **Figure S6. Transcript abundance heatmap for *Ectocarpus* species 7 CAZYme genes**
1030 Heatmaps with $\log_2$(NormalisedCounts+1) for replicate samples of (from left to right) free-swimming
1031 male gamete, sporophyte initial cell (24 hours after gamete release), elongating sporophyte initial
1032 cell (48 hours after gamete release), sporophyte 2-5 cell stage, non-fertile adult sporophyte, fertile
1033 sporophyte, non-fertile female and male gametophyte, fertile female and male gametophyte
1034 *Ectocarpus* species 7 developmental stages for GT23 and PL41 annotated genes. Left annotation
1035 track: differential expression (DEG) analysis results in the transitions between (1) free-swimming
1036 male gamete and sporophyte initial cell stage, and (2) adult sporophyte and gametophyte; right
1037 annotation track: WGCNA module colours.
1038

1039 **Figure S7. Transcript abundance heatmap for *Ectocarpus* species 7 transcription factor genes that**
1040 **have one-to-one *D. dichotoma* orthologues**
1041 Hierarchically clustered heatmap of log_2(NormalisedCounts+1) for 325 *Ectocarpus* species 7 TAP
1042 genes (Denoeud *et al*., 2024) and 90 EsV1-7 domain genes (Macaisne *et al.*, 2017) for replicate
1043 samples of the following life cycle stages: (from left to right) free-swimming male gamete,
1044 sporophyte initial cell (24 hours after gamete release), elongating sporophyte initial cell (48 hours
1045 after gamete release), sporophyte 2-5 cell stage, non-fertile adult sporophyte, fertile sporophyte,
1046 non-fertile female and male gametophytes, fertile female and male gametophytes. Left annotation
1047 track: differential expression (DEG) analysis results in the transitions between 1) free-swimming male
1048 gamete and initial cell stage, and 2) sporophyte and gametophyte; right annotation track: WGCNA
1049 module colours.
1050
1051 **Figure S8. Transcript abundance heatmap for *Ectocarpus* species 7 ribosomal genes**
1052 Heatmap with log_2(NormalisedCounts+1) for (from left to right) free-swimming male gamete,
1053 sporophyte initial cell (24 hours after gamete release), elongating sporophyte initial cell (48 hours
1054 after gamete release), sporophyte 2-5 cell stage, non-fertile adult sporophyte, fertile sporophyte,
1055 non-fertile female and male gametophyte, fertile female and male gametophyte *Ectocarpus* species 7
1056 developmental stages for ribosomal protein annotated genes. Left annotation track: differential
1057 expression analysis results in the transitions between (1) free-swimming male gamete and
1058 sporophyte initial cell stage, and (2) adult sporophyte and gametophyte; right annotation track:
1059 WGCNA module colours.
1060
1061 **Figure S9. Three dimensional representations of a ribosome illustrating differential expression of**
1062 **ribosomal protein genes**
1063 **A., B.** Lateral views. **C.** Top view. **D.** Bottom view. **E. and F.** Intersubunit views of the small and large
1064 subunit, respectively. Small and large subunit ribosomal proteins are coloured in red and purple,
1065 respectively. Darker colour indicates that the gene encoding a protein was significantly upregulated
1066 between the gamete and sporophyte initial cell stages. Proteins coloured in white are present in the
1067 *Triticum aestivum* ribosome, which was used as a reference, but no equivalent was found in
1068 *Ectocarpus* species 7. RNAs are shown as ribbons, ribosomal RNAs in grey, messenger and transfer
1069 RNAs in green. A, P and T indicate the aminoacyl, peptidyl and exit tRNA binding sites, respectively.
1070 En, mRNA entry site; Ex, mRNA exit site; Tu, nascent peptide tunnel exit.
1071
1072 **Figure S10. *D. dichotoma* PCA and modules**
1073 **A.** Principal component analysis of *D. dichotoma* gene expression across seven life cycle stages. **B.**
1074 Characterisation of *D. dichotoma* gene co-expression modules generated using WGCNA. Left to right:
1075 manually-assigned functional categories based on GO term enrichment; number of genes in the
1076 module positively or negatively correlated with the module eigengene; average module gene
1077 expression profiles for WGCNA modules across sperm (1 h after release), egg cell (15 min after
1078 release), zygote (1h after release), embryo (8h after fertilisation), fertile sporophyte, fertile female
1079 and male gametophyte life cycle stages; module eigengene dendrogram. The average module gene
1080 expression profiles were calculated using genes with a WGCNA MM >0.86.
1081
1082 **Figure S11. Enriched GO terms *D. dichotoma* gene modules**
1083 Statistically-significant enriched GO terms in *D. dichotoma* gene modules. Enrichment is indicated as
1084 log2 of the ratio of the proportion of genes assigned to the GO term in the module divided by the
1085 proportion for the whole genome. padj, *p*-value adjusted for multiple testing based on the
1086 Benjamini-Hochberg false discovery rate.
1087
1088 **Figure S12. Transcript abundance heatmap for one-to-one orthologous transcription factors**
1089 **between *Ectocarpus* species 7 and *D. dichotoma***

1090 Heatmap representing expression of one-to-one orthologous genes from *Ectocarpus* species 7 and *D.*
1091 *dichotoma* presented as the z-score of the log_2(NormalisedCounts+1) for the following equivalent
1092 developmental stages in *Ectocarpus* species 7 and *D. dichotoma*: sperm, zygote, early sporophyte,
1093 adult sporophyte, female and male gametophyte. The lefthand tracks show Pearson correlation
1094 coefficients and log_{10} Benjamini-Hochberg-adjusted *p*-values (log10 padj).
1095
1096 **Table S1. RNA-seq data used in this study**
1097 GA, gametophyte; SP, sporophyte, GBG, generation-biased genes.
1098
1099 **Table S2. Generation-biased and generation-specific gene sets in ten species of brown algae based**
1100 **on comparisons of adult sporophyte and gametophyte generations.**
1101 **A.** Overview of the generation-biased and generation-specific gene sets of each species. **B.** Complete
1102 proteomes of the ten species indicating the results of the comparison of adult sporophytes and
1103 gametophytes, including log_2(fold change), *p*-value, mean TPM and assigned generation-biased
1104 expression class. TPM, transcripts per kilobase million.
1105
1106 **Table S3. List of orthogroups for the ten brown algal species analysed for generation-biased gene**
1107 **expression.**
1108 The genomes analysed (with ENA accession numbers or links to ORCAE in brackets) correspond to:
1109 *Dictyota dichotoma* strain ODC1387m (GCA_964200555), *Ectocarpus* species 7 strain Ec32
1110 (https://bioinformatics.psb.ugent.be/orcae/overview/EctsiV2), *Macrocystis pyrifera* strain P11B4
1111 (GCA_964200385), *Myriotrichia clavaeformis* strain Myr cla04 (GCA_964200105), *Pylaiella littoralis*
1112 strain U1.48 (GCA_964200295), *Saccharina latissima* strain SLPER63f7 (GCA_964200175), *Saccharina*
1113 *japonica* strain Ja (https://bioinformatics.psb.ugent.be/orcae/overview/Sacja), *Saccorhiza*
1114 *polyschides* strain SpolBR94m (GCA_964200605), *Scytosiphon promiscuus* strain Ot110409-Otamoi-
1115 16-male (GCA_964200365) and *Sphacelaria rigidula* strain Sph rig Cal Mo 4-1-68b (GCA_964200075).
1116 The one-to-one orthologues correspond to the 9,317 orthogroups identified using the relaxed criteria
1117 described in the Material and Methods.
1118
1119 **Table S4. Counts of RNA-seq reads mapped to *Ectocarpus* species 7 genes**
1120 This data was used to calculate the gene expression levels reported in Table S4.
1121
1122 **Table S5. Functional and expression-related information for *Ectocarpus* species 7 genes**
1123 List of all *Ectocarpus* species 7 genes with transcript abundance under each of the conditions
1124 analysed, measured as log_2(NormalisedCounts +1), WGCNA module assignment (Colour), WGCNA
1125 module membership (MM) scores and associated *p*-values (pMM) for each gene in each module, the
1126 functional annotation for each gene (description), the manually assigned functional category
1127 (Manual.functional.category), the DESeq2 output for the comparison between free-swimming male
1128 gamete and sporophyte initial cell stage (gamete_initial), and adult sporophyte and gametophyte
1129 (sporophyte_gametophyte) with the corresponding differential expression (DE) annotation, the
1130 HECTAR output for each gene with the predicted targeting category and corresponding scores.
1131
1132 **Table S6. Overview of the gene co-expression modules for *Ectocarpus* species 7 and *D. dichotoma***
1133 The grey modules contain all the genes that could not be assigned to a co-expression module. The
1134 gold module was a random sample of 1,000 *Ectocarpus* species 7 genes that provided a null
1135 distribution of gene expression patterns for the comparisons with *D. dichotoma* modules.
1136
1137 **Table S7. Orthofinder orthogroup analysis of *Ectocarpus* species 7 and *D. dichotoma.***
1138 The genomes analysed (with ENA accession numbers or links to ORCAE in brackets) correspond to:
1139 *Dictyota dichotoma* strain ODC1387m (GCA_964200555) and *Ectocarpus* species 7 strain Ec32
1140 (https://bioinformatics.psb.ugent.be/orcae/overview/EctsiV2).
1141

1142 **Table S8. Conservation of life-cycle-related co-expression modules between *Ectocarpus* species 7**
1143 **and *D. dichotoma***
1144 For each *Ectocarpus* species 7 module: preservation statistics computed by the WGCNA
1145 modulePreservation function (200 permutations), preservation statistics computed by the NetRep
1146 modulePreservation function (10,000 permutations) with the associated $\log_{10}$(*p*-value) (Bonferroni-
1147 corrected for WGCNA), and the silhouette score for each module in *D. dichotoma.* WGCNA -
1148 medianRank statistic, aggregation of the densityMedianRank and connectivityMedianRank statistics;
1149 WGCNA – medianRankDensity.pres, WGCNA density median rank preservation statistic; WGCNA –
1150 medianRankConnectivity.pres, WGCNA connectivity median rank preservation statistic; WGCNA -
1151 propVarExplained.pres, coherence: proportion of module variance explained by the module
1152 eigengene (=summary profile = eigenvector of the 1st principal component across all observations
1153 for every node composing the module); WGCNA – meanSignAwareKME.pres, average node
1154 contribution: average Pearson correlation coefficient to the module's summary profile; WGCNA -
1155 meanSignAwareCorDat.pres, density of correlation structure: how strongly modules are correlated in
1156 the test dataset, average node correlation; WGCNA - meanAdj.pres, average edge weight: average
1157 connection strength between nodes; WGCNA – meanMAR.pres, average module adjacency ratio;
1158 WGCNA: cor.kIM, concordance of intramodular connectivity: similarity of the relative rank of each
1159 nodes' weighted degree (intramodular connectivity) across datasets; WGCNA – cor.kME,
1160 concordance of node contribution: preservation of relative rank of nodes (ordered by Pearson
1161 correlation coefficient to the module's summary profile) across datasets; WGCNA – cor.kMEall;
1162 concordance of node contribution: preservation of relative rank of nodes (ordered by Pearson
1163 correlation coefficient to the module's summary profile) across datasets taking into account the kME
1164 of the gene for all modules; WGCNA - cor.cor, concordance of correlation structure: quantifies how
1165 similar the correlation structure is across datasets; WGCNA – cor.MAR, concordance of module
1166 adjacency ratio: concordance of the ration between the maximum and the minimum adjacency in the
1167 module; WGCNA - separability.pres, separability preservation; NetRep - avg.weight, average edge
1168 weight: average connection strength between nodes; NetRep - coherence, coherence, i. e.
1169 proportion of module variance explained by the module eigengene (=summary profile = eigenvector
1170 of the 1st principal component across all observations for every node composing the module);
1171 NetRep – cor.cor, concordance of correlation structure: quantifies how similar the correlation
1172 structure is across datasets; NetRep - cor.degree, concordance of intramodular connectivity:
1173 similarity of the relative rank of each nodes' weighted degree (intramodular connectivity) across
1174 datasets; NetRep - cor.contrib, concordance of node contribution: preservation of relative rank of
1175 nodes (ordered by Pearson correlation coefficient to the module's summary profile) across datasets;
1176 NetRep - avg.cor, density of correlation structure: how strongly modules are correlated in the test
1177 dataset, average node correlation; NetRep - avg.contrib, average node contribution: average Pearson
1178 correlation coefficient to the module's summary profile; silhouette.cluster.width, Silhouette
1179 coefficient; silhouette.distance.to.average, Silhouette coefficient. The "gold" module was a random
1180 sample of 1,000 *Ectocarpus* species 7 genes that provided a control distribution of gene expression
1181 patterns for comparisons with *D. dichotoma* modules. The "darkturquoise" module was not included
1182 in this analysis because it contained zero orthologues (Table S5).
1183
1184 **Table S9. Counts of RNA-seq reads mapped to *D. dichotoma* genes**
1185 This data was used to calculate the gene expression levels reported in Table S8.
1186
1187 **Table S10. Functional and expression-related information for *D. dichotoma* genes**
1188 List of all *D. dichotoma* genes with the $\log_2$(NormalisedCounts+1) under each condition used for the
1189 analysis, WGCNA module assignment (Colour), WGCNA module membership (MM) scores and
1190 associated *p*-values (pMM) for each gene in each module.
1191
1192 **Table S11. Correlation between the expression patterns of orthologous transcription factors in**
1193 ***Ectocarpus* species 7 and *D. dichotoma***

1194 Correlation was evaluated based on comparisons six approximately equivalent stages for the two
1195 species (Table S1). The names of the *Ectocarpus* species 7 and *D. dichotoma* genes in each
1196 orthogroup are given in Figure S12. padj, *p*-value adjusted for multiple testing based on the
1197 Benjamini-Hochberg false discovery rate.
1198
1199 **Table S12. Manual re-annotation of the *Ectocarpus* species 7 ribosomal proteins.**
1200 The e-values and scores are for BLASTp queries of the *Ectocarpus* species 7 ribosomal proteins
1201 against the *Arabidopsis thaliana* ribosomal protein dataset.
1202
1203 **References**
1204

1205 Ahmed S, Cock JM, Pessia E, Luthringer R, Cormier A, Robuchon M, Sterck L, Peters AF, Dittami SM,
1206 Corre E, Valero M, Aury JM, Roze D, Van de Peer Y, Bothwell J, Marais GA, Coelho SM (2014)
1207 A Haploid System of Sex Determination in the Brown Alga *Ectocarpus* sp. **Curr Biol** 24:1945–
1208 1957.

1209 Akita S, Vieira C, Hanyuda T, Rousseau F, Cruaud C, Couloux A, Heesch S, Cock JM, Kawai H (2022)
1210 Providing a phylogenetic framework for trait-based analyses in brown algae: Phylogenomic
1211 tree inferred from 32 nuclear protein-coding sequences. **Molecular Phylogenetics and**
1212 **Evolution** 168:107408.

1213 Al-Hinai TZS, Mackay CL, Fry SC (2024) Fruit softening: evidence for rhamnogalacturonan lyase action
1214 *in vivo* in ripe fruit cell walls. **Annals of Botany** 133:547–558.

1215 Anderson SN, Johnson CS, Chesnut J, Jones DS, Khanday I, Woodhouse M, Li C, Conrad LJ, Russell SD,
1216 Sundaresan V (2017) The Zygotic Transition Is Initiated in Unicellular Plant Zygotes with
1217 Asymmetric Activation of Parental Genomes. **Dev Cell** 43:349-358.e4.

1218 Andrews S (2016) FastQC A Quality Control tool for High Throughput Sequence Data.
1219 **http://www.bioinformatics.babraham.ac.uk/projects/fastqc/**.

1220 Arun A, Coelho SM, Peters AF, Bourdareau S, Pérès L, Scornet D, Strittmatter M, Lipinska AP, Yao H,
1221 Godfroy O, Montecinos GJ, Avia K, Macaisne N, Troadec C, Bendahmane A, Cock JM (2019)
1222 Convergent recruitment of TALE homeodomain life cycle regulators to direct sporophyte
1223 development in land plants and brown algae. **Elife** 8:e43101.

1224 Arun A, Peters NT, Scornet D, Peters AF, Cock JM, Coelho SM (2013) Non-cell autonomous regulation
1225 of life cycle transitions in the model brown alga *Ectocarpus*. **New Phytol** 197:503–510.

1226 Bacher R, Leng N, Chu L-F, Ni Z, Thomson JA, Kendziorski C, Stewart R (2018) Trendy: segmented
1227 regression analysis of expression dynamics in high-throughput ordered profiling experiments.
1228 **BMC Bioinformatics** 19:380.

1229 Bogaert KA, Beeckman T, De Clerck O (2017) Two-step cell polarization in algal zygotes. **Nat Plants**
1230 3:16221.

1231 Bourdareau S, Tirichine L, Lombard B, Loew D, Scornet D, Wu Y, Coelho SM, Cock JM (2021) Histone
1232 modifications during the life cycle of the brown alga *Ectocarpus*. **Genome Biology** 22:12.

1233 Bringloe TT, Starko S, Wade RM, Vieira C, Kawai H, Clerck OD, Cock JM, Coelho SM, Destombe C,
1234 Valero M, Neiva J, Pearson GA, Faugeron S, Serrão EA, Verbruggen H (2020) Phylogeny and
1235 Evolution of the Brown Algae. **Critical Reviews in Plant Sciences** 39:281–321.

1236 Carvalho-Santos Z, Azimzadeh J, Pereira-Leal JB, Bettencourt-Dias M (2011) Evolution: Tracing the
1237 origins of centrioles, cilia, and flagella. **J Cell Biol** 194:165–175.

1238 Chen J, Strieder N, Krohn NG, Cyprys P, Sprunck S, Engelmann JC, Dresselhaus T (2017) Zygotic
1239 Genome Activation Occurs Shortly after Fertilization in Maize. **The Plant Cell** 29:2106–2125.

1240 Choi S-W, Graf L, Choi JW, Jo J, Boo GH, Kawai H, Choi CG, Xiao S, Knoll AH, Andersen RA, Yoon HS
1241 (2024) Ordovician origin and subsequent diversification of the brown algae. **Curr Biol**:S0960-
1242 9822(23)01769-4.

1243 Choksi SP, Lauter G, Swoboda P, Roy S (2014) Switching on cilia: transcriptional networks regulating
1244 ciliogenesis. **Development** 141:1427–1441.

1245 Chu JSC, Baillie DL, Chen N (2010) Convergent evolution of RFX transcription factors and ciliary genes
1246 predated the origin of metazoans. **BMC Evol Biol** 10:130.

1247 Cock JM et al. (2010) The *Ectocarpus* genome and the independent evolution of multicellularity in
1248 brown algae. **Nature** 465:617–621.

1249 Cock JM, Godfroy O, Macaisne N, Peters AF, Coelho SM (2014) Evolution and regulation of complex
1250 life cycles: a brown algal perspective. **Curr Opin Plant Biol** 17:1–6.

1251 Coelho SM, Cock JM (2020) Brown algal model organisms. **Ann Rev Genet** 54:71–92.

1252 Coelho SM, Godfroy O, Arun A, Le Corguillé G, Peters AF, Cock JM (2011) *OUROBOROS* is a master
1253 regulator of the gametophyte to sporophyte life cycle transition in the brown alga
1254 *Ectocarpus*. **Proc Natl Acad Sci USA** 108:11518–11523.

1255 Coelho SM, Scornet D, Rousvoal S, Peters N, Dartevelle L, Peters AF, Cock JM (2012a) Genetic crosses
1256 between *Ectocarpus* strains. **Cold Spring Harb Protoc** 2012:262–265.

1257 Coelho SM, Scornet D, Rousvoal S, Peters NT, Dartevelle L, Peters AF, Cock JM (2012b) How to
1258 cultivate *Ectocarpus*. **Cold Spring Harb Protoc** 2012:258–261.

1259 Cormier A, Avia K, Sterck L, Derrien T, Wucher V, Andres G, Monsoor M, Godfroy O, Lipinska A,
1260 Perrineau M-M, Van De Peer Y, Hitte C, Corre E, Coelho SM, Cock JM (2017) Re-annotation,
1261 improved large-scale assembly and establishment of a catalogue of noncoding loci for the
1262 genome of the model brown alga *Ectocarpus*. **New Phytol** 214:219–232.

1263 Danecek P, Bonfield JK, Liddle J, Marshall J, Ohan V, Pollard MO, Whitwham A, Keane T, McCarthy SA,
1264 Davies RM, Li H (2021) Twelve years of SAMtools and BCFtools. **Gigascience** 10:giab008.

1265 Denoeud F et al. (2024) Evolutionary genomics of the emergence of brown algae as key components
1266 of coastal ecosystems. **Cell** 187:6943–6965.

1267 Dopler A et al. (2024) P-stalk ribosomes act as master regulators of cytokine-mediated processes. **Cell**
1268 Available at: https://www.sciencedirect.com/science/article/pii/S0092867424011395
1269 [Accessed November 25, 2024].

1270 Eger AM, Marzinelli EM, Beas-Luna R, Blain CO, Blamey LK, Byrnes JEK, Carnell PE, Choi CG, Hessing-
1271 Lewis M, Kim KY, Kumagai NH, Lorda J, Moore P, Nakamura Y, Pérez-Matus A, Pontier O,
1272 Smale D, Steinberg PD, Vergés A (2023) The value of ecosystem services in global marine kelp
1273 forests. **Nat Commun** 14:1894.

1274 Emms DM, Kelly S (2019) OrthoFinder: phylogenetic orthology inference for comparative genomics.
1275 **Genome Biol** 20:238.

1276 Godfroy O, Uji T, Nagasato C, Lipinska AP, Scornet D, Peters AF, Avia K, Colin S, Mignerot L,
1277 Motomura T, Cock JM, Coelho SM (2017) DISTAG/TBCCd1 Is Required for Basal Cell Fate
1278 Determination in *Ectocarpus*. **Plant Cell** 29:3102–3122.

1279 Godfroy O, Zheng M, Yao H, Henschen A, Peters AF, Scornet D, Colin S, Ronchi P, Hipp K, Nagasato C,
1280 Motomura T, Cock JM, Coelho SM (2023) The *baseless* mutant links protein phosphatase 2A
1281 with basal cell identity in the brown alga *Ectocarpus*. **Development** 150:dev201283.

1282 Gogala M, Becker T, Beatrix B, Armache J-P, Barrio-Garcia C, Berninghausen O, Beckmann R (2014)
1283 Structures of the Sec61 complex engaged in nascent peptide translocation or membrane
1284 insertion. **Nature** 506:107–110.

1285 Graf L, Shin Y, Yang JH, Hwang IK, Yoon HS (2022) Transcriptome analysis reveals the spatial and
1286 temporal differentiation of gene expression in the sporophyte of *Undaria pinnatifida*. **Algal**
1287 **Research** 68:102883.

1288 Gschloessl B, Guermeur Y, Cock J (2008) HECTAR: a method to predict subcellular targeting in
1289 heterokonts. **BMC Bioinf** 9:393.

1290 Hoshino M, Kogame K (2019) Parthenogenesis is rare in the reproduction of a sexual field population
1291 of the isogamous brown alga Scytosiphon (Scytosiphonaceae, Ectocarpales). **J Phycol** 55:466–
1292 472.

1293 Inoue A, Ojima T (2019) Functional identification of alginate lyase from the brown alga Saccharina
1294 japonica. **Sci Rep** 9:4937.

1295 Kim D, Paggi JM, Park C, Bennett C, Salzberg SL (2019) Graph-based genome alignment and
1296 genotyping with HISAT2 and HISAT-genotype. **Nat Biotechnol** 37:907–915.

1297 Kolde R (2019) Pheatmap: pretty heatmaps. **R package version** 1:726.

1298 Krueger F (2015) Trim Galore!: A wrapper around Cutadapt and FastQC to consistently apply adapter
1299 and quality trimming to FastQ files, with extra functionality for RRBS data. **Babraham**
1300 **Institute** Available at: https://cir.nii.ac.jp/crid/1370294643762929691 [Accessed October 8,
1301 2024].

1302 Langfelder P, Horvath S (2008) WGCNA: an R package for weighted correlation network analysis.
1303 **BMC Bioinformatics** 9:559.

1304 Lawrence M, Gentleman R, Carey V (2009) rtracklayer: an R package for interfacing with genome
1305 browsers. **Bioinformatics** 25:1841–1842.

1306 Li L, Tian G, Peng H, Meng D, Wang L, Hu X, Tian C, He M, Zhou J, Chen L, Fu C, Zhang W, Hu Z (2018)
1307 New class of transcription factors controls flagellar assembly by recruiting RNA polymerase II
1308 in *Chlamydomonas*. **Proc Natl Acad Sci U S A** 115:4435–4440.

1309 Liang Z, Wang X, Zhang P, Liu W, Wang W, Liu F (2023) Chronological development of the
1310 morphological, physiological, biochemical, and transcriptomic changes provides insights into
1311 the mechanisms of gametogenesis in Saccharina japonica. **J Appl Phycol** 35:785–802.

1312 Liao Y, Smyth GK, Shi W (2014) featureCounts: an efficient general purpose program for assigning
1313 sequence reads to genomic features. **Bioinformatics** 30:923–930.

1314 Lipinska AP, Serrano-Serrano ML, Cormier A, Peters AF, Kogame K, Cock JM, Coelho SM (2019) Rapid
1315 turnover of life-cycle-related genes in the brown algae. **Genome Biol** 20:35.

1316 Love MI, Huber W, Anders S (2014) Moderated estimation of fold change and dispersion for RNA-seq
1317 data with DESeq2. **Genome Biol** 15:550.

1318 Lüdecke D (2018) sjmisc: Data and Variable Transformation Functions. **Journal of Open Source**
1319 **Software** 3:754.

1320 Macaisne N, Liu F, Scornet D, Peters AF, Lipinska A, Perrineau M-M, Henry A, Strittmatter M, Coelho
1321 SM, Cock JM (2017) The *Ectocarpus IMMEDIATE UPRIGHT* gene encodes a member of a novel
1322 family of cysteine-rich proteins with an unusual distribution across the eukaryotes.
1323 **Development** 144:409–418.

1324 Martin DE, Soulard A, Hall MN (2004) TOR regulates ribosomal protein gene expression via PKA and
1325 the Forkhead transcription factor FHL1. **Cell** 119:969–979.

1326 Mazéas L, Bouguerba-Collin A, Cock JM, Denoeud F, Godfroy O, Brillet-Guéguen L, Barbeyron T,
1327 Lipinska AP, Delage L, Corre E, Drula E, Henrissat B, Czjzek M, Terrapon N, Hervé C (2024)
1328 Candidate genes involved in biosynthesis and degradation of the main extracellular matrix
1329 polysaccharides of brown algae and their probable evolutionary history. **BMC Genomics**
1330 25:950.

1331 Méndez-Yañez A, González M, Carrasco-Orellana C, Herrera R, Moya-León MA (2020) Isolation of a
1332 rhamnogalacturonan lyase expressed during ripening of the Chilean strawberry fruit and its
1333 biochemical characterization. **Plant Physiology and Biochemistry** 146:411–419.

1334 Meng EC, Goddard TD, Pettersen EF, Couch GS, Pearson ZJ, Morris JH, Ferrin TE (2023) UCSF
1335 ChimeraX: Tools for structure building and analysis. **Protein Science** 32:e4792.

1336 Müller DG (1967) Generationswechsel, Kernphasenwechsel und Sexualität der Braunalge *Ectocarpus*
1337 *siliculosus* im Kulturversuch. **Planta** 75:39–54.

1338 Ni C, Buszczak M (2023) The homeostatic regulation of ribosome biogenesis. **Semin Cell Dev Biol**
1339 136:13–26.

1340 Pearson GA, Martins N, Madeira P, Serrão EA, Bartsch I (2019) Sex-dependent and -independent
1341 transcriptional changes during haploid phase gametogenesis in the sugar kelp Saccharina
1342 latissima. **PLOS ONE** 14:e0219723.

1343 Peters AF, Scornet D, Ratin M, Charrier B, Monnier A, Merrien Y, Corre E, Coelho SM, Cock JM (2008)
1344 Life-cycle-generation-specific developmental processes are modified in the *immediate*
1345 *upright* mutant of the brown alga *Ectocarpus siliculosus*. **Development** 135:1503–1512.

1346 Ritchie SC, Watts S, Fearnley LG, Holt KE, Abraham G, Inouye M (2016) A Scalable Permutation
1347 Approach Reveals Replication and Preservation Patterns of Network Modules in Large
1348 Datasets. **cels** 3:71–82.

1349 Scarpin MR, Busche M, Martinez RE, Harper LC, Reiser L, Szakonyi D, Merchante C, Lan T, Xiong W,
1350 Mo B, Tang G, Chen X, Bailey-Serres J, Browning KS, Brunkard JO (2023) An updated
1351 nomenclature for plant ribosomal protein genes. **The Plant Cell** 35:640–643.

1352 Shan T, Li Q, Wang X, Pang S (2020) Full-length transcriptome sequencing and comparative
1353 transcriptomic analysis of different developmental stages of the sporophyll in Undaria
1354 pinnatifida (Laminariales: Alariaceae). **J Appl Phycol** 32:2081–2092.

1355 Shao Z, Zhang P, Lu C, Li S, Chen Z, Wang X, Duan D (2019) Transcriptome sequencing of Saccharina
1356 japonica sporophytes during whole developmental periods reveals regulatory networks
1357 underlying alginate and mannitol biosynthesis. **BMC Genomics** 20:975.

1358 Starr RC, Zeikus JA (1993) UTEX-The culture collection of algae at the University of Texas at Austin
1359 1993 list of cultures. **J Phycol** 29 (Suppl.):1–106.

1360 Sterck L, Billiau K, Abeel T, Rouzé P, Van de Peer Y (2012) ORCAE: online resource for community
1361 annotation of eukaryotes. **Nat Methods** 9:1041.

1362 Tadros W, Lipshitz HD (2009) The maternal-to-zygotic transition: a play in two acts. **Development**
1363 136:3033–3042.

1364 Uji T, Kandori T, Mizuta H (2024) Identification of differential gene expression related to reproduction
1365 in the sporophytes of Saccharina japonica. **Front Plant Sci** 15 Available at:
1366 https://www.frontiersin.org/journals/plant-science/articles/10.3389/fpls.2024.1417582/full
1367 [Accessed November 20, 2024].

1368 Uluisik S, Seymour GB (2020) Pectate lyases: Their role in plants and importance in fruit ripening.
1369 **Food Chemistry** 309:125559.

1370 van den Hoek C, Mann DG, Jahns HM (1995) Algae: An Introduction to Phycology. Cambridge:
1371 Cambridge University Press.

1372 Vastenhouw NL, Cao WX, Lipshitz HD (2019) The maternal-to-zygotic transition revisited.
1373 **Development** 146:dev161471.

1374 Wang P, Hendron R-W, Kelly S (2017) Transcriptional control of photosynthetic capacity:
1375 conservation and divergence from *Arabidopsis* to rice. **New Phytol** 216:32–45.

1376 Waters MT, Wang P, Korkaric M, Capper RG, Saunders NJ, Langdale JA (2009) GLK transcription
1377 factors coordinate expression of the photosynthetic apparatus in *Arabidopsis*. **Plant Cell**
1378 21:1109–1128.

1379 Wawiórka L, Molestak E, Szajwaj M, Michalec-Wawiórka B, Mołoń M, Borkiewicz L, Grela P,
1380 Boguszewska A, Tchórzewski M (2017) Multiplication of Ribosomal P-Stalk Proteins
1381 Contributes to the Fidelity of Translation. **Molecular and Cellular Biology** 37:e00060-17.

1382 Wickham H, Averick M, Bryan J, Chang W, McGowan LD, François R, Grolemund G, Hayes A, Henry L,
1383 Hester J (2019) Welcome to the Tidyverse. **Journal of open source software** 4:1686.

1384 Wickham H, Chang W, Wickham MH (2016) Package 'ggplot2.' **Create elegant data visualisations**
1385 **using the grammar of graphics Version** 2:1–189.

1386 Xu T, Le TD, Liu L, Su N, Wang R, Sun B, Colaprico A, Bontempi G, Li J (2017) CancerSubtypes: an
1387 R/Bioconductor package for molecular cancer subtype identification, validation and
1388 visualization. **Bioinformatics** 33:3131–3133.

1389 Xue Z, Huang K, Cai C, Cai L, Jiang C, Feng Y, Liu Z, Zeng Q, Cheng L, Sun YE, Liu J, Horvath S, Fan G
1390 (2013) Genetic programs in human and mouse early embryos revealed by single-cell RNA
1391 sequencing. **Nature** 500:593–597.

1392 Yao H, Scornet D, Jam M, Hervé C, Potin P, Correia LO, Coelho SM, Cock JM (2021) Biochemical
1393 characteristics of a diffusible factor that induces gametophyte to sporophyte switching in the
1394 brown alga *Ectocarpus*. **Journal of Phycology** 57:742–753.

1395 Yu G, Wang L-G, Han Y, He Q-Y (2012) clusterProfiler: an R package for comparing biological themes
1396 among gene clusters. **OMICS** 16:284–287.

1397 Zhang J, Li Y, Luo S, Cao M, Zhang L, Li X (2021) Differential gene expression patterns during
1398 gametophyte development provide insights into sex differentiation in the dioicous kelp
1399 Saccharina japonica. **BMC Plant Biol** 21:335.

1400 Zhao P, Zhou X, Shen K, Liu Z, Cheng T, Liu D, Cheng Y, Peng X, Sun M-X (2019) Two-Step Maternal-to-
1401 Zygotic Transition with Two-Phase Parental Genome Contributions. **Dev Cell** 49:882-893.e5.

1402

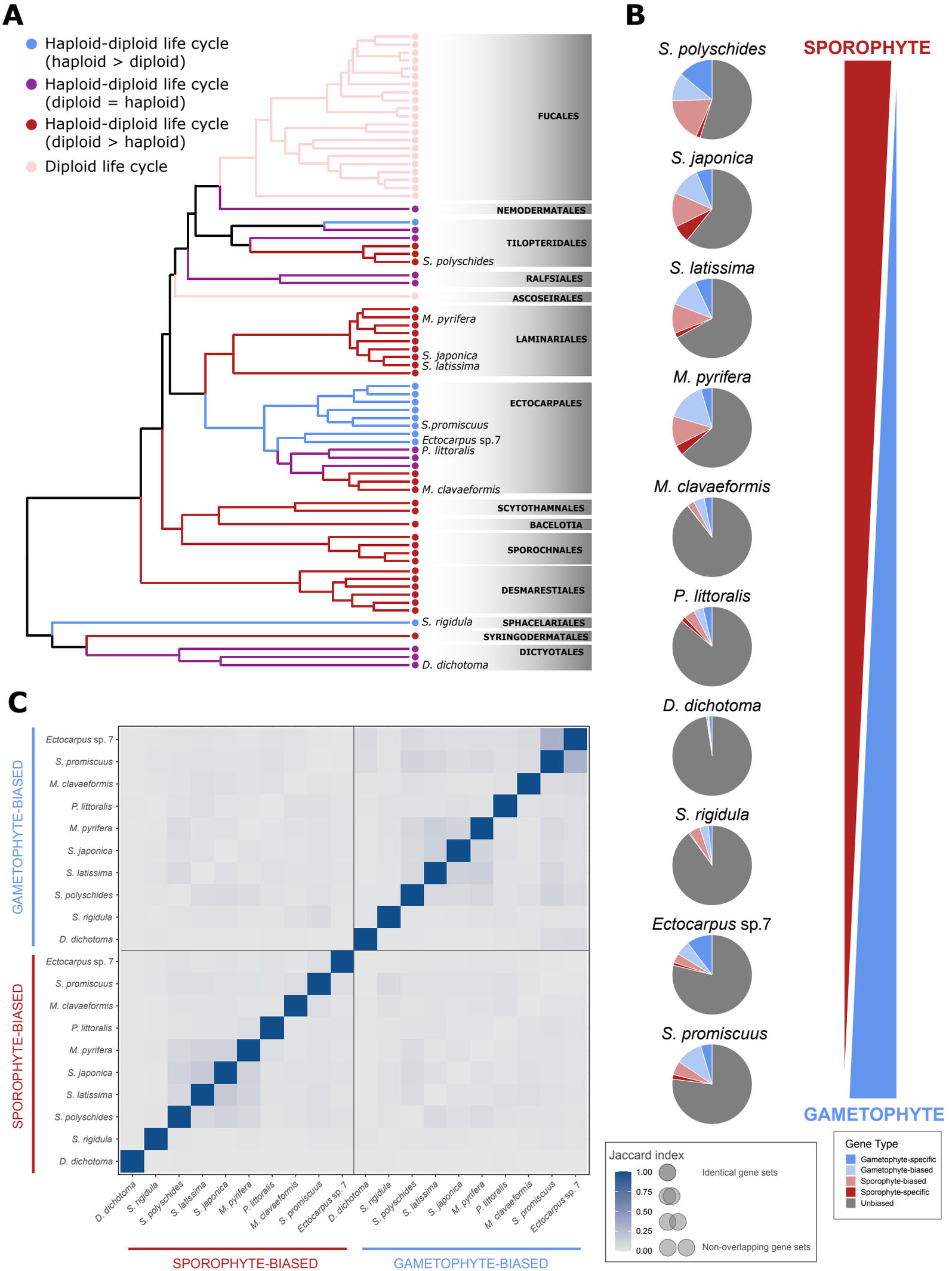
A
Haploid-diploid life cycle (haploid > diploid)
Haploid-diploid life cycle (diploid = haploid)
Haploid-diploid life cycle (diploid > haploid)
Diploid life cycle
FUCALES
NEMODERMATALES
TILOPTERIDALES
S. polyschides
RALFSIALES
ASCOSEIRALES
M. pyrifera
LAMINARIALES
S. japonica
S. latissima
ECTOCARPALES
S.promiscuus
Ectocarpus sp.7
P. littoralis
M. clavaeformis
SCYTOTHAMNALES
BACELOTIA
SPOROCHNALES
DESMARESTIALES
S. rigidula
SPHACELARIALES
SYRINGODERMATALES
DICTYOTALES
D. dichotoma
B
S. polyschides
S. japonica
S. latissima
M. pyrifera
M. clavaeformis
P. littoralis
D. dichotoma
S. rigidula
Ectocarpus sp.7
S. promiscuus
SPOROPHYTE
GAMETOPHYTE
C
GAMETOPHYTE-BIASED
SPOROPHYTE-BIASED
Ectocarpus sp. 7
S. promiscuus
M. clavaeformis
P. littoralis
M. pyrifera
S. japonica
S. latissima
S. polyschides
S. rigidula
D. dichotoma
SPOROPHYTE-BIASED
GAMETOPHYTE-BIASED
Jaccard index
1.00
0.75
0.50
0.25
0.00
Identical gene sets
Non-overlapping gene sets
Gene Type
Gametophyte-specific
Gametophyte-biased
Sporophyte-biased
Sporophyte-specific
Unbiased

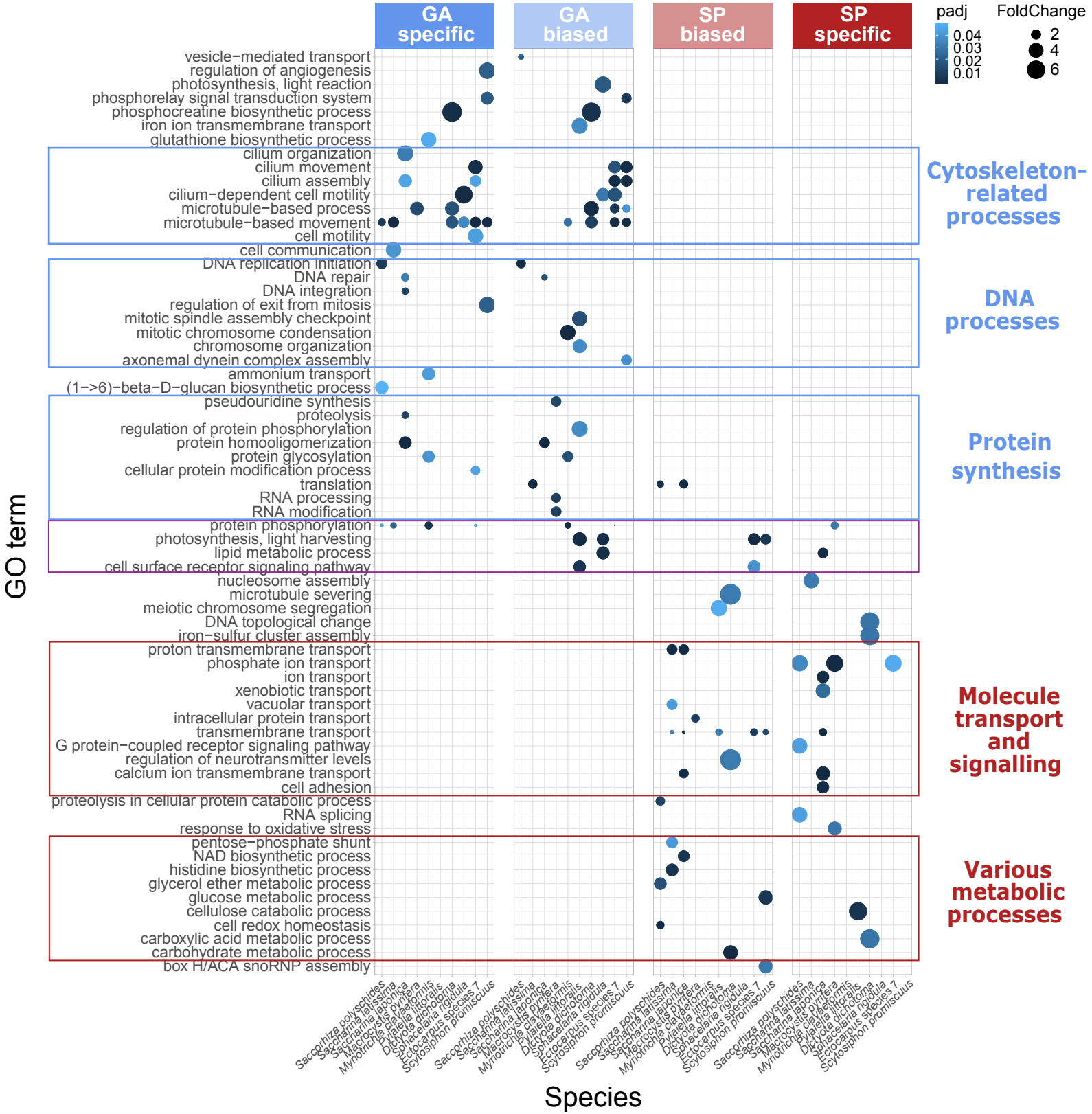
GA specific
GA biased
SP biased
SP specific
padj
0.04
0.03
0.02
0.01
FoldChange
2
4
6
GO term
vesicle−mediated transport
regulation of angiogenesis
photosynthesis, light reaction
phosphorelay signal transduction system
phosphocreatine biosynthetic process
iron ion transmembrane transport
glutathione biosynthetic process
cilium organization
cilium movement
cilium assembly
cilium−dependent cell motility
microtubule−based process
microtubule−based movement
cell motility
cell communication
DNA replication initiation
DNA repair
DNA integration
regulation of exit from mitosis
mitotic spindle assembly checkpoint
mitotic chromosome condensation
chromosome organization
axonemal dynein complex assembly
ammonium transport
(1−>6)−beta−D−glucan biosynthetic process
pseudouridine synthesis
proteolysis
regulation of protein phosphorylation
protein homooligomerization
protein glycosylation
cellular protein modification process
translation
RNA processing
RNA modification
protein phosphorylation
photosynthesis, light harvesting
lipid metabolic process
cell surface receptor signaling pathway
nucleosome assembly
microtubule severing
meiotic chromosome segregation
DNA topological change
iron−sulfur cluster assembly
proton transmembrane transport
phosphate ion transport
ion transport
xenobiotic transport
vacuolar transport
intracellular protein transport
transmembrane transport
G protein−coupled receptor signaling pathway
regulation of neurotransmitter levels
calcium ion transmembrane transport
cell adhesion
proteolysis in cellular protein catabolic process
RNA splicing
response to oxidative stress
pentose−phosphate shunt
NAD biosynthetic process
histidine biosynthetic process
glycerol ether metabolic process
glucose metabolic process
cellulose catabolic process
cell redox homeostasis
carboxylic acid metabolic process
carbohydrate metabolic process
box H/ACA snoRNP assembly
Cytoskeleton-related processes
DNA processes
Protein synthesis
Molecule transport and signalling
Various metabolic processes
Saccorhiza polyschides
Saccharina latissima
Saccharina japonica
Macrocystis pyrifera
Myriotrichia clavaeformis
Dictyota dichotoma
Pylaiella littoralis
Sphacelaria rigidula
Ectocarpus species 7
Scytosiphon promiscuus
Species

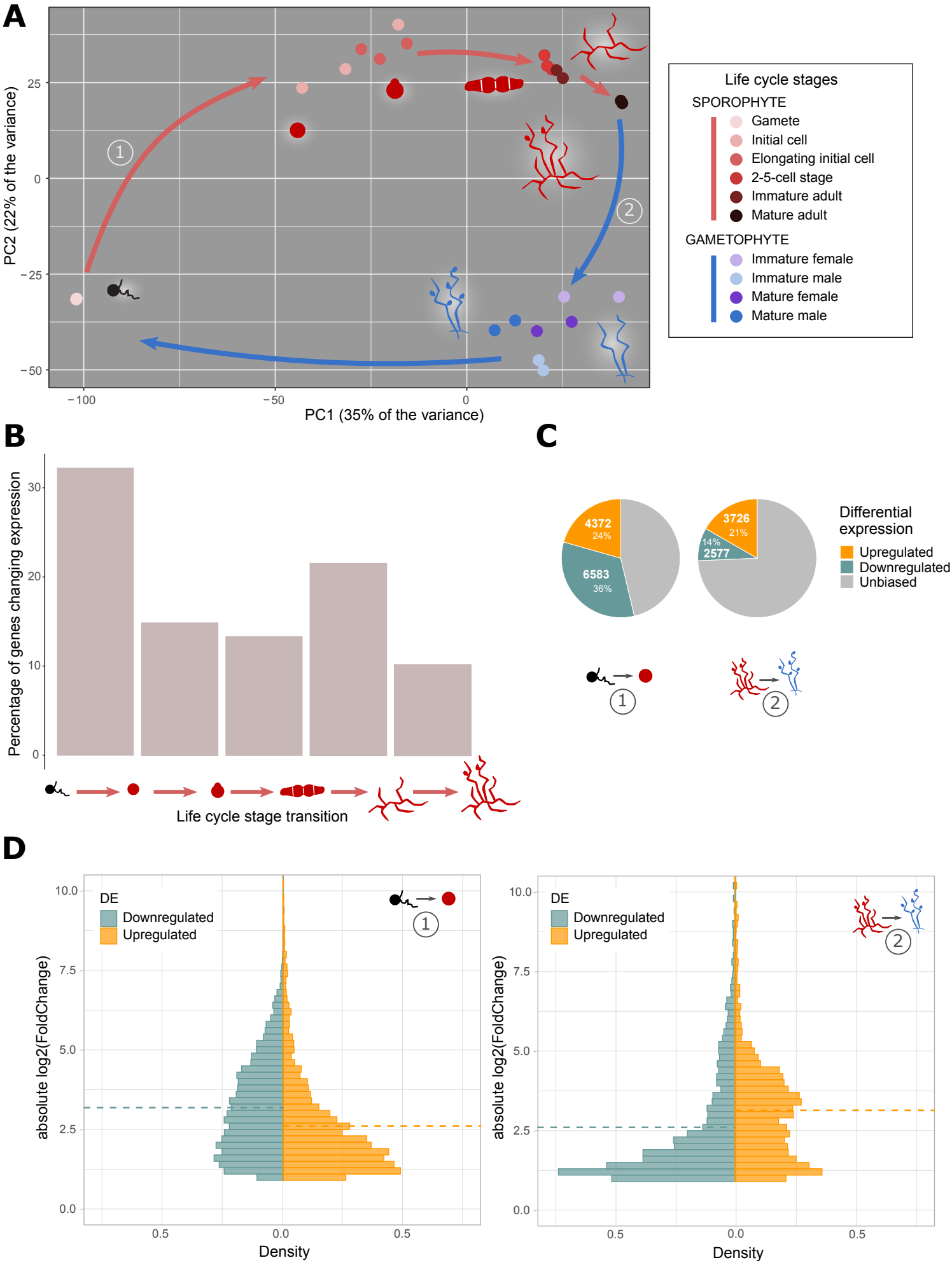
A
PC2 (22% of the variance)
PC1 (35% of the variance)
25
0
−25
−50
−100
−50
0
1
2
Life cycle stages
SPOROPHYTE
Gamete
Initial cell
Elongating initial cell
2-5-cell stage
Immature adult
Mature adult
GAMETOPHYTE
Immature female
Immature male
Mature female
Mature male
B
Percentage of genes changing expression
30
20
10
0
Life cycle stage transition
C
4372
24%
6583
36%
3726
21%
14%
2577
Differential expression
Upregulated
Downregulated
Unbiased
1
2
D
DE
Downregulated
Upregulated
absolute log2(FoldChange)
10.0
7.5
5.0
2.5
0.0
0.5
0.0
0.5
Density
1
2

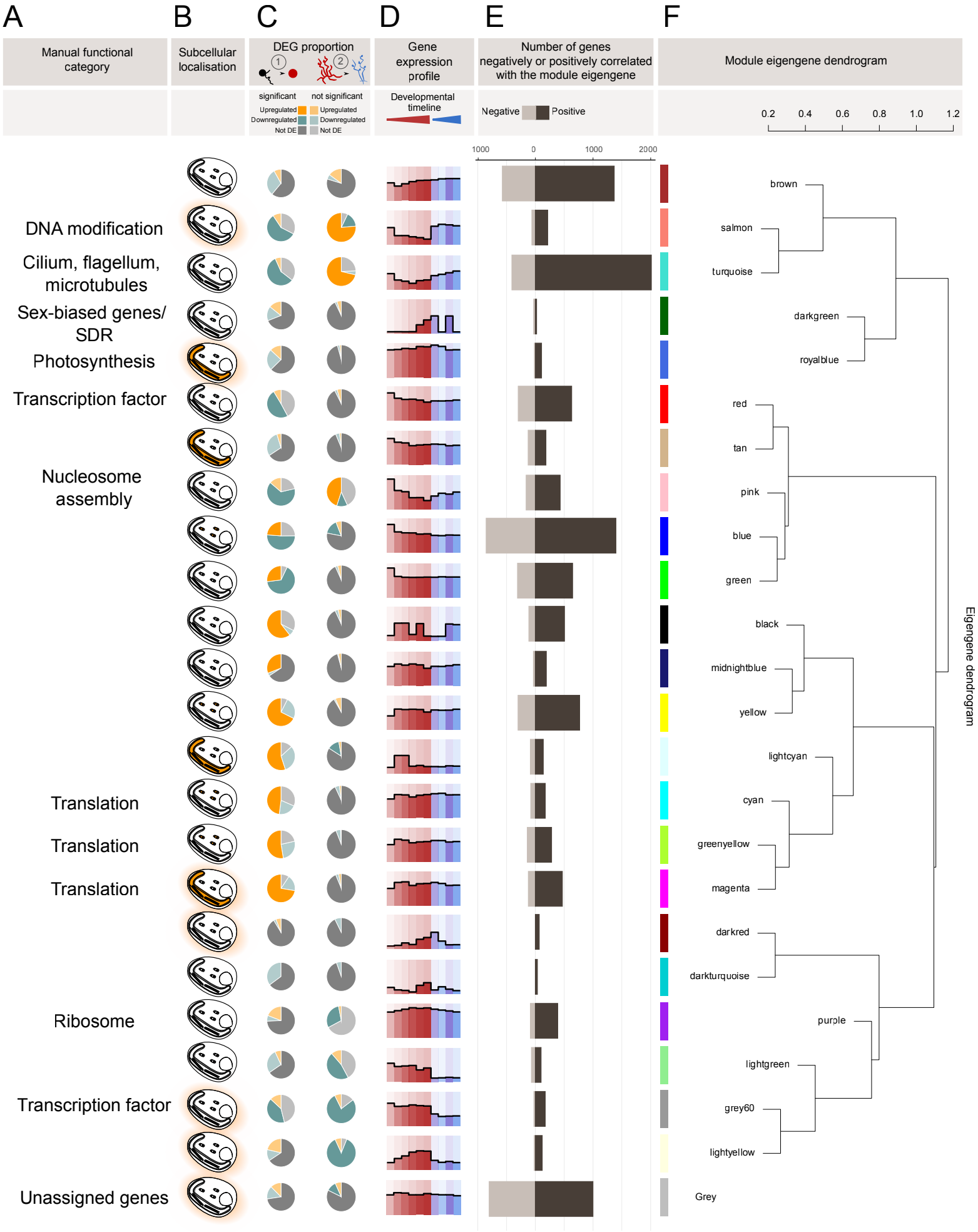
A
B
C
D
E
F
Manual functional category
Subcellular localisation
DEG proportion
Gene expression profile
Number of genes negatively or positively correlated with the module eigengene
Module eigengene dendrogram
significant
not significant
Upregulated
Downregulated
Not DE
Developmental timeline
Negative
Positive
0.2
0.4
0.6
0.8
1.0
1.2
1000
0
1000
2000
DNA modification
Cilium, flagellum, microtubules
Sex-biased genes/ SDR
Photosynthesis
Transcription factor
Nucleosome assembly
Translation
Translation
Translation
Ribosome
Transcription factor
Unassigned genes
brown
salmon
turquoise
darkgreen
royalblue
red
tan
pink
blue
green
black
midnightblue
yellow
lightcyan
cyan
greenyellow
magenta
darkred
darkturquoise
purple
lightgreen
grey60
lightyellow
Grey
Eigengene dendrogram

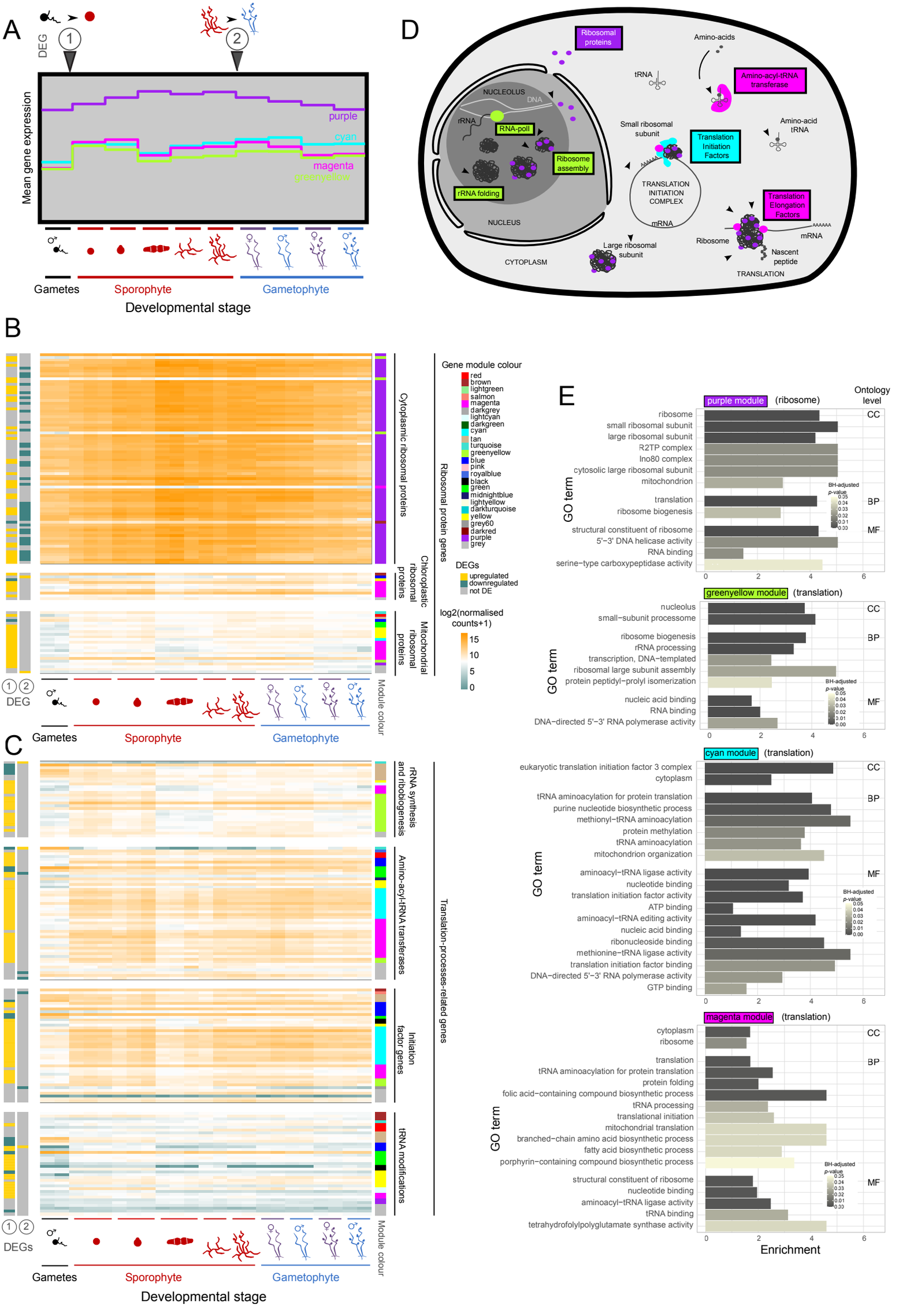
A
DEG
1
2
Mean gene expression
purple
cyan
magenta
greenyellow
Gametes
Sporophyte
Gametophyte
Developmental stage
D
Ribosomal proteins
Amino-acids
tRNA
Amino-acyl-tRNA transferase
NUCLEOLUS
DNA
rRNA
RNA-poll
Small ribosomal subunit
Translation Initiation Factors
Amino-acid tRNA
Ribosome assembly
TRANSLATION INITIATION COMPLEX
rRNA folding
Translation Elongation Factors
NUCLEUS
mRNA
Ribosome
Large ribosomal subunit
Nascent peptide
CYTOPLASM
TRANSLATION
B
Cytoplasmic ribosomal proteins
Chloroplastic ribosomal proteins
Mitochondrial ribosomal proteins
Ribosomal protein genes
Module colour
Gene module colour
red
brown
lightgreen
salmon
magenta
darkgrey
lightcyan
darkgreen
cyan
tan
turquoise
greenyellow
blue
pink
royalblue
black
green
midnightblue
lightyellow
darkturquoise
yellow
grey60
darkred
purple
grey
DEGs
upregulated
downregulated
not DE
log2(normalised counts+1)
15
10
5
0
C
rRNA synthesis and ribobiogenesis
Amino-acyl-tRNA transferases
Initiation factor genes
tRNA modifications
Translation-processes-related genes
DEGs
E
purple module (ribosome)
Ontology level
CC
BP
MF
GO term
ribosome
small ribosomal subunit
large ribosomal subunit
R2TP complex
Ino80 complex
cytosolic large ribosomal subunit
mitochondrion
translation
ribosome biogenesis
structural constituent of ribosome
5'−3' DNA helicase activity
RNA binding
serine−type carboxypeptidase activity
BH-adjusted p-value
greenyellow module (translation)
nucleolus
small−subunit processome
ribosome biogenesis
rRNA processing
transcription, DNA−templated
ribosomal large subunit assembly
protein peptidyl−prolyl isomerization
nucleic acid binding
RNA binding
DNA−directed 5'−3' RNA polymerase activity
cyan module (translation)
eukaryotic translation initiation factor 3 complex
cytoplasm
tRNA aminoacylation for protein translation
purine nucleotide biosynthetic process
methionyl−tRNA aminoacylation
protein methylation
tRNA aminoacylation
mitochondrion organization
aminoacyl−tRNA ligase activity
nucleotide binding
translation initiation factor activity
ATP binding
aminoacyl−tRNA editing activity
nucleic acid binding
ribonucleoside binding
methionine−tRNA ligase activity
translation initiation factor binding
DNA−directed 5'−3' RNA polymerase activity
GTP binding
magenta module (translation)
cytoplasm
ribosome
translation
tRNA aminoacylation for protein translation
protein folding
folic acid−containing compound biosynthetic process
tRNA processing
translational initiation
mitochondrial translation
branched−chain amino acid biosynthetic process
fatty acid biosynthetic process
porphyrin−containing compound biosynthetic process
structural constituent of ribosome
nucleotide binding
aminoacyl−tRNA ligase activity
tRNA binding
tetrahydrofolylpolyglutamate synthase activity
Enrichment

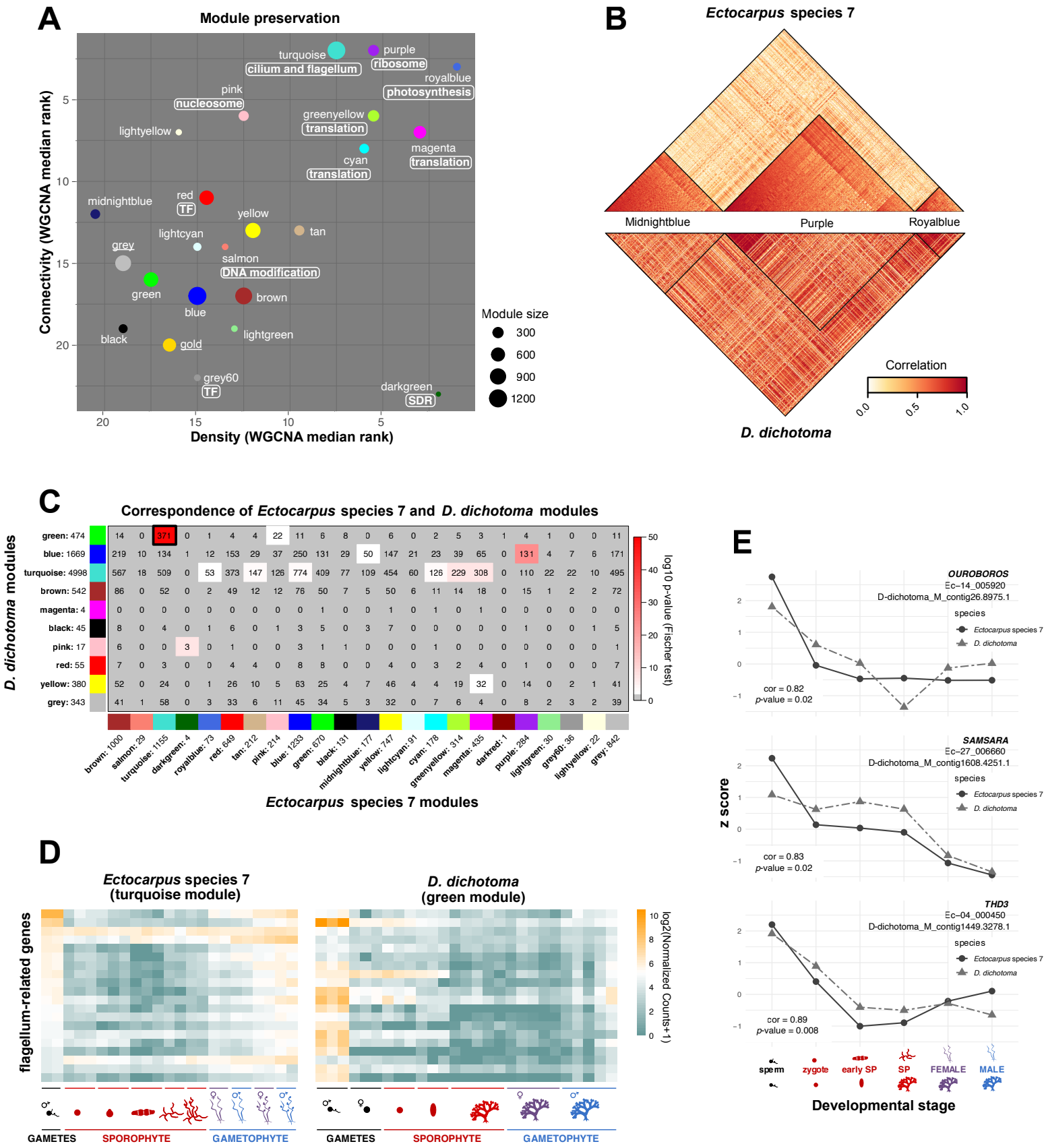
A
Module preservation
Connectivity (WGCNA median rank)
Density (WGCNA median rank)
turquoise
cilium and flagellum
purple
ribosome
royalblue
photosynthesis
pink
nucleosome
greenyellow
translation
lightyellow
magenta
translation
cyan
translation
midnightblue
red
TF
yellow
tan
lightcyan
grey
salmon
DNA modification
green
brown
blue
black
lightgreen
gold
grey60
TF
darkgreen
SDR
Module size
300
600
900
1200
B
Ectocarpus species 7
Midnightblue
Purple
Royalblue
Correlation
0.0
0.5
1.0
D. dichotoma
C
Correspondence of Ectocarpus species 7 and D. dichotoma modules
D. dichotoma modules
green: 474
blue: 1669
turquoise: 4998
brown: 542
magenta: 4
black: 45
pink: 17
red: 55
yellow: 380
grey: 343
brown: 1000
salmon: 29
turquoise: 1155
darkgreen: 4
royalblue: 73
red: 649
tan: 212
pink: 214
blue: 1233
green: 670
black: 131
midnightblue: 177
yellow: 747
lightcyan: 91
cyan: 178
greenyellow: 314
magenta: 435
darkred: 1
purple: 284
lightgreen: 30
grey60: 36
lightyellow: 22
grey: 842
log10 p-value (Fischer test)
Ectocarpus species 7 modules
D
Ectocarpus species 7
(turquoise module)
D. dichotoma
(green module)
flagellum-related genes
log2(Normalized Counts+1)
GAMETES
SPOROPHYTE
GAMETOPHYTE
E
OUROBOROS
Ec–14_005920
D-dichotoma_M_contig26.8975.1
species
Ectocarpus species 7
D. dichotoma
cor = 0.82
p-value = 0.02
SAMSARA
Ec–27_006660
D-dichotoma_M_contig1608.4251.1
cor = 0.83
p-value = 0.02
THD3
Ec–04_000450
D-dichotoma_M_contig1449.3278.1
cor = 0.89
p-value = 0.008
z score
sperm
zygote
early SP
SP
FEMALE
MALE
Developmental stage